

# Multi-particle and inclusive reactions

A. K. Likhoded and P. V. Shlyapnikov

*Institute of High Energy Physics, Serpukhov*  
Usp. Fiz. Nauk **124**, 3-59 (January 1978)

Recent experimental data on inclusive particle yields in hadron-hadron interactions are analyzed from the point of view of their scale-invariant properties. It is shown that the hypothesis of limiting fragmentation does not hold over the entire range of accelerator energies, although it is consistent with the data at the highest energies, where it is satisfied to an accuracy of 3-20%. The energy dependence of inclusive reactions is in agreement with the predictions of Mueller-Regge phenomenology. Factorization of the leading Regge singularities is confirmed to an accuracy of at least 10% for many reactions. The observed violation of Feynman's scaling law for the central region of the inclusive spectrum at the highest CERN ISR energies is consistent with the existence of a constant limit as  $s \rightarrow \infty$  and a certain factorization property. Models which relate hadron-hadron interactions to deep inelastic scattering processes are discussed. An important feature of these considerations is that they allow for the contributions from resonance decays in the stable-particle spectra. The experimental situation regarding the yields of resonances is analyzed in the light of the quark-parton picture.

PACS numbers: 13.85.Kf, 12.40.Mm, 11.80.Cr

## CONTENTS

1. Introduction. . . . .	1
2. Notation and Inclusive Sum Rules . . . . .	2
3. Total Inclusive Cross Sections . . . . .	4
4. Regularities in the Approach to Scaling and Inclusive Distributions . . . . .	5
5. Inclusive Resonance Production. . . . .	16
6. Conclusions. . . . .	26
References. . . . .	26

## 1. INTRODUCTION

The aim of the present review is to provide an exposition of the basic experimental results obtained from studies of multi-particle processes at high energies. The global description of multi-particle processes in the framework of the inclusive approach formulated by Logunov *et al.*,<sup>[1]</sup> the first experimental evidence for the existence of scale invariance in hadronic interactions,<sup>[2,3]</sup> and its theoretical reinterpretation in terms of the hypotheses of limiting fragmentation<sup>[4]</sup> and scaling<sup>[5]</sup> have stimulated a vigorous development of this area of high-energy physics and have helped to make it possible to obtain a vast number of experimental and theoretical results that have significantly deepened our understanding of the mechanisms of multi-particle production processes.

Many important results were presented at the recent 18th International Conference on High Energy Physics at Tbilisi. For example, a dramatic violation of scaling in the central region has been reliably established in experiments over the wide range of energies from several GeV to 2000 GeV. It has been convincingly demonstrated that the production of the observed particles in multi-particle reactions takes place mainly via the formation and subsequent decay of resonances. Thus it appears that clustering and short-range correlation effects can be explained to a great extent by the production of resonances. Many experimental results suggest that there exists a deep analogy between processes involving strong, electromagnetic, and weak interactions at high

energies.

Owing to the abundance of experimental data, it is not possible to consider all aspects of the physics of multi-particle processes within the scope of a single review. We shall therefore concentrate on the most recent results obtained from studies of multi-particle and inclusive reactions in the light of the reviews presented at the Tbilisi conference. The inevitable gaps in our exposition can be filled by a number of detailed reviews.<sup>[6-11]</sup> The present survey is based on recent review talks,<sup>[12-14]</sup> which in some cases contain more complete experimental data and more detailed bibliographies.

In Sec. 2 we introduce our notation and consider inclusive sum rules and the consequences of the experimentally established growth of the total cross sections with energy and of the hypothesis of scale invariance. In Sec. 3 we discuss the experimental data on the total inclusive cross sections for pions and neutral strange particles in hadron-hadron interactions and their energy dependences. Section 4 is devoted to the regularities in the approach to scaling in the fragmentation regions of the incident particles and in the central region, and to the inclusive single-particle distributions. The energy dependences of the inclusive cross sections in the various kinematic regions are compared with various theoretical predictions. We discuss experiments to test factorization of the leading Regge singularities, transverse scaling, and the relationship between inclusive reactions and deep inelastic scattering. The inclusive production of meson and baryon resonances is the sub-

ject of Sec. 5. The experimental data are compared with the predictions of quark models, and the characteristic properties of the inclusive distributions of resonances and their production mechanisms are discussed. A brief summary of the main results is given in the concluding section.

## 2. NOTATION AND INCLUSIVE SUM RULES

In the past few years, studies of single-particle and two-particle inclusive reactions

$$a + b \rightarrow c + X, \quad (2.1)$$

$$a + b \rightarrow c_1 + c_2 + X, \quad (2.2)$$

in which analyses are made of the distributions of one or two particles, while an integration is carried out over all the other particles of the system  $X$ , have become one of the principal methods of investigating multi-particle processes. These reactions are described by means of the invariant distribution functions

$$f(p_c, s) = E_c \frac{d^3\sigma}{d^3p_c}, \quad (2.3)$$

$$f_2(p_1, p_2, s) = E_1 E_2 \frac{d^6\sigma}{d^3p_1 d^3p_2}. \quad (2.4)$$

In addition, two-particle inclusive reactions are characterized by the correlation function

$$c_2(p_1, p_2, s) = \rho_2(p_1, p_2, s) - \rho(p_1, s)\rho(p_2, s), \quad (2.5)$$

where  $\rho_2(p_1, p_2, s) = f_2(p_1, p_2, s)/\sigma_{\text{tot}}$  and  $\rho(p_1, s) = f(p_1, s)/\sigma_{\text{tot}}$  are the two-dimensional and one-dimensional distribution densities, respectively.<sup>1)</sup>

Integrating (2.3)–(2.5) with respect to the appropriate Lorentz-invariant phase space  $E_c^{-1}d^3p_c$  or  $E_1^{-1}E_2^{-1}d^3p_1 \times d^3p_2$ , we obtain the relations

$$\int d^3p_c E_c^{-1} f(p_c, s) = \langle n_c \rangle \sigma_{\text{tot}}, \quad (2.6)$$

$$\int d^3p_1 d^3p_2 E_1^{-1} E_2^{-1} f_2(p_1, p_2, s) = \langle n_1 n_2 - n_1 \delta_{12} \rangle \sigma_{\text{tot}}, \quad (2.7)$$

$$\int d^3p_1 d^3p_2 E_1^{-1} E_2^{-1} c_2(p_1, p_2, s) = \langle n_1 n_2 - n_1 \delta_{12} \rangle - \langle n_1 \rangle \langle n_2 \rangle. \quad (2.8)$$

The integral (2.6) is called the total inclusive cross section for the particle  $c$  in the reaction (2.1); the integral (2.8) is known as the integrated correlation parameter and is equal to  $\langle n(n-1) \rangle - \langle n \rangle^2$  when the particles  $c_1$  and  $c_2$  in the reaction (2.2) are identical. Kinematic correlations due to the laws of energy and momentum conservation lead to non-zero values of the integrated correlation parameter even in the absence of dynamical correlations between the particles.

In experiments involving unpolarized particles, owing to the azimuthal symmetry of the interaction with respect to the direction of the incident particles, the distribution function  $f(p, s)$  at fixed total c. m. energy  $\sqrt{s}$

<sup>1)</sup> Instead of normalizing to the total cross section  $\sigma_{\text{tot}}$  in (2.5)–(2.8), it is possible to adopt a normalization to the total inelastic cross section  $\sigma_{\text{inel}}$ , or to the cross section  $\sigma_{\text{inel}}(c)$  for only those events in which particles of type  $c$  are produced. In this case,  $\langle n_c \rangle$  is the average multiplicity of particles of type  $c$  for inelastic events or for those events in which only the particles  $c$  are produced.

TABLE I.

Variables	$p, \Omega$	$p_L, p_T^2$	$x, p_T^2$	$y, p_T^2$	$M^2, t$
$f(p, s)$	$\frac{E}{p^2} \frac{d^2\sigma}{d p d\Omega}$	$\frac{E}{\pi} \frac{d^2\sigma}{d p_T^2 d p_L}$	$\frac{E}{\pi p_{\text{max}}} \frac{d^2\sigma}{d p_T^2 d x}$	$\frac{1}{\pi} \frac{d^2\sigma}{d p_T^2 d y}$	$\frac{d^2\sigma}{\pi d t d (M^2/s)}$

depends only on two variables. The most frequently used sets of variables and the corresponding expressions for  $f(p, s)$  are given in Table I. Here  $p, p_L, p_T$ , and  $\Omega$  are respectively the magnitude and the longitudinal and transverse components of the momentum  $\mathbf{p}$  of the inclusive particle and its solid angle, which, together with the rapidity  $y = \frac{1}{2} \ln[(E + p_L)/(E - p_L)]$ , can be defined in the c. m. s., in the laboratory system, or in the rest system of the incident particle. The transverse mass  $m_T = \sqrt{p_T^2 + m_c^2}$  is often used instead of the variable  $p_T$ . The scaling variable  $x = p_L/p_{\text{max}} \approx 2p_L/\sqrt{s}$  is defined in the c. m. s.;  $M^2 = (p_a + p_b - p_c)^2$  is the square of the missing mass corresponding to the particle  $c$  in the reaction (2.1), and  $t = (p_a - p_c)^2$  is the square of the 4-momentum transferred to this particle.

The distribution function  $f_2(p_1, p_2, s)$  and the correlation function  $C_2(p_1, p_2, s)$  for the two-particle inclusive reaction (2.2) at fixed  $s$  depend on five variables. When experimental data or theoretical predictions are presented, an integration is usually carried out with respect to most of the variables over their entire range of variation or over certain intervals. For example, the inclusive production of resonance states is studied by analyzing the spectra of effective masses  $M_{12}^2 = (p_1 + p_2)^2$  of two particles. Two-particle correlations are studied in the space of rapidities  $y_1$  and  $y_2$  of the two particles; correlations in the azimuthal angle  $\varphi_{12} = \arccos(\mathbf{p}_{T1}\mathbf{p}_{T2}/p_{T1}p_{T2})$  between the transverse momenta are studied.

Equations (2.6)–(2.8) are the simplest examples of so-called inclusive sum rules. In addition, there also exist energy sum rules,<sup>[15]</sup> which take the following form for the invariant distribution functions  $f(p, s)$  and  $f(p_1, p_2, s)$  for the reactions (2.1) and (2.2):

$$\sum_c \int d^3p_c E_c^{-1} p_c^\mu f(p_c, s) = (p_a + p_b)^\mu \sigma_{\text{tot}}, \quad (2.9)$$

$$\sum_{c_1, c_2} \int d^3p_1 d^3p_2 E_1^{-1} E_2^{-1} p_1^\mu p_2^\nu f_2(p_1, p_2, s) = (p_a + p_b)^\mu (p_a + p_b)^\nu \sigma_{\text{tot}} - \sum_{c_1} \int d^3p_2 E_2^{-1} p_2^\mu p_1^\nu f(p_2, s). \quad (2.10)$$

The summations in (2.9) and (2.10) are taken over all types of particles in the reactions (2.1) and (2.2), and  $\mu$  is an index which labels the 4-momentum components of a particle. We shall consider several important consequences of the inclusive sum rules (2.6)–(2.10), the growth of the total cross sections, and the hypothesis of scale invariance.

The law of conservation of energy [ $p^4 = E_c$  in (2.9)] leads to the following relation, which holds in the c. m. s.:

$$\sum_c \int d^3p_c f(p_c, s) = \sqrt{s} \sigma_{\text{tot}}. \quad (2.11)$$

Defining the inelasticity coefficient  $\eta_c$  as the fraction of

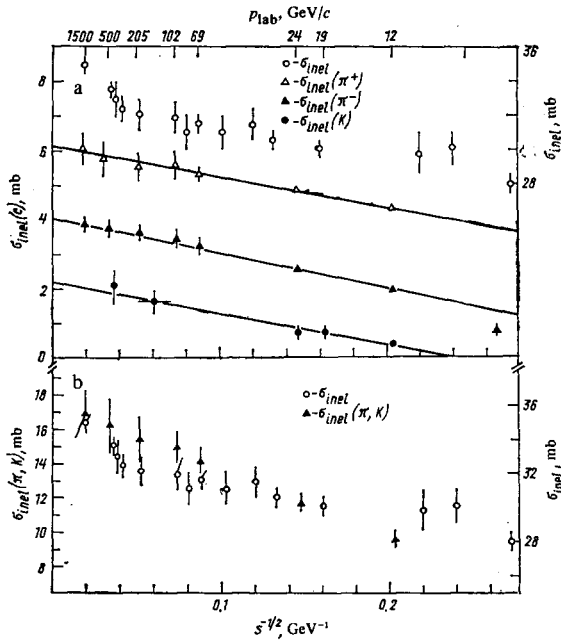


FIG. 1. The energy dependences of the total inelastic cross section (right-hand scale) and of the contributions to the total inelastic cross section from  $\sigma_{inel}(\pi^+)$ ,  $\sigma_{inel}(\pi^-)$ ,  $\sigma_{inel}(K^+, K^-, K^0, \bar{K}^0)$  (left-hand scale) (a) and of the total inelastic cross section (right-hand scale) and the total contribution to  $\sigma_{inel}$  from  $\pi^+$ ,  $\pi^-$ ,  $\pi^0$ ,  $K^+$ ,  $K^-$ ,  $K^0$ ,  $\bar{K}^0$  (left-hand scale) (b).<sup>[20]</sup>

the total energy  $\sqrt{s}$  carried away by the particles of type  $c$ , we have

$$\eta_c = \frac{1}{\sqrt{s} \sigma_{tot}} \int d^3 p_c f(p_c, s). \quad (2.12)$$

In the variables  $x$  and  $p_T^2$ , Eq. (2.11) takes the form

$$\frac{\pi}{2} \sum_c \int dx_c dp_{Tc}^2 f(x_c, p_{Tc}^2, s) = \sigma_{tot}. \quad (2.13)$$

Thus Eq. (2.13) gives a direct relation between the energy dependence of the total (inelastic) cross sections and the corresponding behavior of the invariant distribution functions for the inclusive reactions.

The growth of the total cross sections, which was first established at Serpukhov and which is known as the Serpukhov effect, is often associated with an entirely new class of phenomena which have no analog at low energies and which are due to the appearance of a new energy scale resulting from the production of heavy particles with masses of order 3–5 GeV.<sup>[16]</sup> According to models<sup>[17]</sup> in which Froissart's upper bound is saturated, the total cross section in the FNAL-ISR energy range grows like

$$\sigma_{tot} = \sigma_0 + \sigma_1 \ln^2 \left( \frac{s}{s_0} \right), \quad (2.14)$$

and contains a scale parameter  $s_0 \approx 120 \text{ GeV}^2$ , which determines the threshold energy for a new mechanism involving maximum saturation of the partial waves.

One might attempt to attribute this threshold behavior of the total cross section to the energy dependence of the invariant inclusive distribution. In this connection, it

is of interest to examine the relation between the observed growth of the total cross sections and the hypothesis of scale invariance,<sup>[5]</sup> which asserts that there exists an  $s$ -independent asymptotic limit for the distribution function  $f(p, s)$  as  $s \rightarrow \infty$ :

$$f(x, p_T^2, s) \xrightarrow{s \rightarrow \infty} f^\infty(x, p_T^2). \quad (2.15)$$

This limit might set in earlier for inclusive reactions involving light particles and later for reactions involving heavy particles, thus leading to an effective growth of  $\sigma_{tot}$  with increasing energy. On the other hand, studies of the energy dependences of the inclusive distributions in various kinematic regions may also throw light on the possible mechanisms for producing a growth of  $\sigma_{tot}$  at the highest accelerator energies. Thus, it was once popular to attribute the growth of  $\sigma_{inel}$  to the growth of the inclusive cross sections for protons near the kinematic boundary  $1 - |x| \ll 1$  (the triple-reggeon region). An integration of the invariant inclusive distributions over the region  $|x| \geq 0.94$  actually leads to a growth of the cross section like  $\ln s$  or  $\ln \ln s$ , depending on the behavior of the triple-pomeron vertex near  $t=0$ .<sup>[18]</sup> However, owing to the peak for  $|x| \rightarrow 1$ , this growth is compensated by the falling-off of the proton spectrum for small values of  $x$  in the fragmentation region, so that the total contribution turns out to be practically independent of energy.<sup>[19]</sup> In addition, as can be seen from Fig. 1, the absolute growth of  $\sigma_{inel}$  for  $p\bar{p}$  interactions over the energy range 24–1500 GeV can be fully explained by the growth of the total contribution to  $\sigma_{inel}$  from  $\sigma_{inel}(\pi)$  and  $\sigma_{inel}(K)$ , which, as we shall show below, is due to the growth of the inclusive cross sections for pions and kaons in the central region.

By applying the scaling hypothesis (2.15) to the inclusive sum rule (2.6), we can predict the asymptotic energy dependence of the total inclusive cross sections. In fact,

$$\sigma_c = \int d^3 p E^{-1} f(p, s) \xrightarrow{s \rightarrow \infty} \pi \int dx dp_T^2 \frac{f^\infty(x, p_T^2)}{\sqrt{x^2 + (4m_T^2/s)}}. \quad (2.16)$$

Owing to the boundedness of the distribution  $f^\infty(x, p_T^2)$  with respect to the transverse momenta, at sufficiently high energies (2.16) can be represented in the following form, which is accurate up to the first term of the expansion:

$$\sigma_c \xrightarrow{s \rightarrow \infty} \pi \left[ \int dp_T^2 f^\infty(0, p_T^2) \right] \ln s + O(\ln s).$$

Thus, for a non-zero value of the integral at  $x=0$ , the hypothesis of scale invariance leads to a logarithmic growth of the total inclusive cross sections with energy:

$$\sigma_c = A_\infty + B_\infty \ln s, \quad (2.17)$$

where

$$B_\infty = \pi \int dp_T^2 f^\infty(0, p_T^2).$$

When applied to the inclusive sum rule (2.7) for the two-particle inclusive reaction and the analogous sum rules for the complete set of  $k$ -particle inclusive reac-

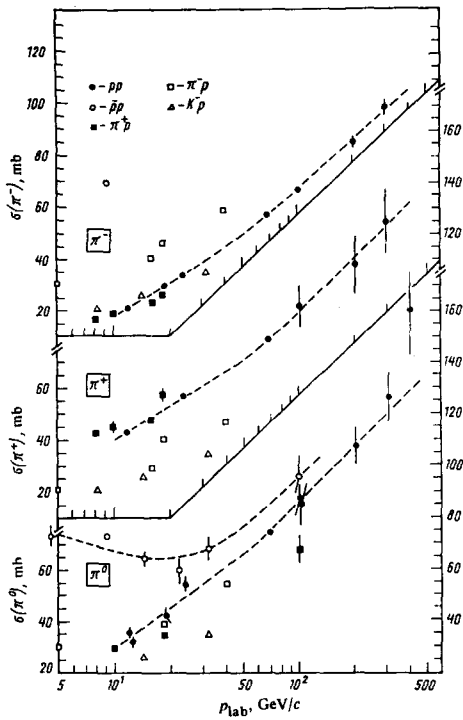


FIG. 2. Inclusive cross sections for  $\pi^+$ ,  $\pi^-$ , and  $\pi^0$  mesons as a function of the primary momentum. The points show a compilation<sup>[12]</sup> of published data; the lines are drawn by eye through the experimental points.

tions, the hypothesis of scale invariance makes it possible to obtain a scaling result for the multiplicity distributions of secondary charged particles<sup>[21]</sup>:

$$\frac{\langle n \rangle \sigma_n}{\sigma_{\text{inel}}} = \psi \left( \frac{n}{\langle n \rangle} \right), \quad (2.18)$$

where  $\sigma_n$  are the topological cross sections, and  $\psi(n/\langle n \rangle)$  is a certain universal function which describes the data over a wide range of energies and which has little dependence on the type of incident particle (for details, see, e.g., Ref. 10).

Thus scale invariance leads to a number of important predictions for the energy dependences of the multiplicity distributions, of the total inclusive cross sections, and of the invariant distribution functions in inclusive reactions, thereby restricting the class of possible theoretical models, while the inclusive sum rules relate the energy dependences of the cross sections for inclusive processes to the total interaction cross sections for the particles. The growth of the total cross sections and the observed violation of scaling within the accessible range of energies make it all the more necessary to carry out careful experimental investigations of the energy dependences of inclusive processes in various kinematic regions.

### 3. TOTAL INCLUSIVE CROSS SECTIONS

Recent data on the energy dependences of the total inclusive cross sections for  $\pi^+$ ,  $\pi^-$ , and  $\pi^0$  mesons,  $\sigma_\pi = \langle n_\pi \rangle \sigma_{\text{inel}}$ , are compiled in Fig. 2. The growth in the cross sections for pions in  $pp$  interactions above 50 GeV/c is in agreement with a logarithmic dependence,

TABLE II. Total inclusive cross sections  $\sigma$  (mb) for  $\pi^+$ ,  $\pi^-$ , and  $\pi^0$  mesons in  $pp$  and  $Kp$  interactions at high energies.

$p_{\text{lab}}$ , GeV/c	pp				K-p	
	6932	10010	20510, 23	30310, 24	1487	3220
$\sigma(\pi^+)$	$78.5 \pm 1.3$	$91.8 \pm 9.2$	$108 \pm 11$	$125 \pm 13$	$25.6 \pm 0.8$	$33.6 \pm 1.3$
$\sigma(\pi^-)$	$57.5 \pm 0.6$	$66.9 \pm 1.3$	$86 \pm 2$	$99.5 \pm 3$	$25.9 \pm 1.5$	$36.3 \pm 1.8$
$\sigma(\pi^0)$	$74.0 \pm 1.5$	$85 \pm 8$	$107 \pm 7$	$126.5 \pm 9$	$27.2 \pm 1.0$	$35.3 \pm 0.8$

which, however, does not fit the energy dependences of the cross sections over the entire range of accelerator energies. The contribution to the total inclusive cross section for pions from the fragmentation component<sup>2)</sup> is still important even at FNAL energies, as can be seen from the appreciable difference between the cross sections for producing particles and antiparticles (Table II). For example, the ratio of cross sections  $\sigma(\pi^-)/\sigma(\pi^+)$  varies slowly from  $0.74 \pm 0.02$  at 69 GeV/c<sup>[24]</sup> to  $0.80 \pm 0.08$  at 303 GeV/c.<sup>[10]</sup> Since the closeness of the ratio  $\sigma_\pi/\sigma_c$  to unity can be regarded as a measure of the approach to a regime involving a limiting logarithmic growth, it follows from the experimental data that the limiting logarithmic regime (2.17) has not yet become established at currently accessible energies. However, the coefficient of the  $\ln s$  term in (2.17) must evidently have a value appreciably larger than that obtained from simple logarithmic fits to the existing data.

The energy dependence of the cross sections for pions in reactions involving other beam particles is similar to that observed in  $pp$  interactions, but the difference in the quantum numbers of the initial particles shows up in the energy dependence of the cross sections for pions, at least for energies up to 100 GeV, and can be attributed to the operation of the conservation laws, the effects of the leading particles, and the contribution from the annihilation channels. Thus, the inclusive cross sections for  $\pi^0$  mesons in  $\bar{p}p$  interactions up to the Serpukhov energies fall off markedly with increasing primary momenta as a result of the decreasing contribution from the annihilation channel. In the interval of primary momenta from 22.4 to 100 GeV/c, the cross sections for mesons begin to rise with increasing energy at about the same rate as in  $pp$  interactions, since for momenta above 100 GeV/c the contribution from the annihilation component is less than 5% of the total cross section for  $\bar{p}p$  interactions.

Figures 3 and 4 show the behavior of the cross sections for producing the neutral strange particles  $K^0$ ,  $\Lambda$ , and  $\bar{\Lambda}$ . The cross sections for neutral strange kaons in  $pp$  interactions rise by an order of magnitude over the range of primary momenta from 12 GeV/c to the maximum values available at FNAL, while in the case of  $\pi^+p$  interactions the energy dependence of the cross section for producing  $K^0$  mesons is consistent with a logarithmic behavior over the entire range of momenta up to 205 GeV/c.<sup>[27]</sup> The cross sections for  $K^0$  mesons in  $\bar{p}p$  interactions are systemati-

<sup>2)</sup>The term "fragmentation component" henceforth implies that part of the inclusive cross section corresponding to fixed values of the variable  $x$  ( $|x| > 0$ ) of the inclusive particle.

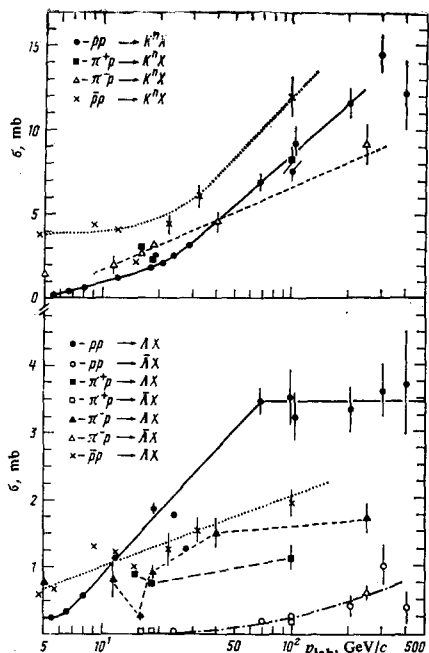


FIG. 3. The  $K^n$ ,  $\Lambda$ , and  $\bar{\Lambda}$  inclusive cross sections as a function of the primary momentum for  $p^+p$  and  $\pi^+p$  interactions. The points are from a compilation<sup>[12]</sup> of published data; the lines are drawn by eye through the experimental points.

cally higher than in the case of  $pp$  interactions, and in the Serpukhov-FNAL energy range they rise as rapidly as in the case of  $pp$  collisions.

The cross section for producing  $\Lambda$  hyperons in  $pp$  interactions rises within the range of momenta from 5 to 50 GeV/c but varies little at higher energies. Starting with the Serpukhov energies,  $\sigma(\Lambda)$  is approximately twice as large in  $pp$  as in  $\bar{p}p$  and  $\pi^+p$  interactions, as is to be expected if the dominant process for producing  $\Lambda$  hyperons is proton fragmentation. The dominance of the fragmentation process over the central production of  $\Lambda\bar{\Lambda}$  pairs also explains the weak dependence of the cross sections for producing  $\Lambda$  hyperons in the FNAL energy range. The cross section for  $\bar{\Lambda}$  production is small, but it rises strongly with energy for  $p_{lab} > 69$  GeV/c, in analogy with the behavior of the antiproton yields.

The cross sections for producing neutral strange particles, measured by the France-USSR and CERN-USSR Collaboration in  $K^+p$  interactions at 32 GeV/c, are compared with the corresponding data at lower energies in Fig. 4. In both  $K^+p$  and  $K^-p$  collisions, we find an appreciable growth of the cross sections for  $K^n$  mesons,  $\Delta\sigma \approx 1.5$  mb, over the range from 16 to 32 GeV/c. This growth may be at least partially explained by the large cross sections for producing  $K^n K^n$  pairs:  $\sigma(K^n \bar{K}^n) = 1.1 \pm 0.1$  mb and  $1.68 \pm 0.24$  mb in  $K^+p$ <sup>[32]</sup> and  $K^-p$ <sup>[25]</sup> interactions at 32 GeV/c, respectively. It is interesting to note that a similar growth of  $K^+K^-$  pair production has been observed in the exclusive reaction channels in  $K^+p$  collisions at 32 GeV/c.<sup>[33]</sup> An analogous effect has also been seen in  $K^-p$  collisions at 32 GeV/c<sup>[34]</sup>:

$$\frac{\sigma(K^-p \rightarrow K^-pK^+K^-\pi^+\pi^-)}{\sigma(K^-p \rightarrow K^-p2\pi^+2\pi^-)} = 0.18 \pm 0.05,$$

$$\frac{\sigma(K^-p \rightarrow K^-pK^+K^-2\pi^+2\pi^-)}{\sigma(K^-p \rightarrow K^-p3\pi^+3\pi^-)} = 0.55 \pm 0.21.$$

The energy dependence of the  $\Lambda$  and  $\bar{\Lambda}$  cross sections in  $K^+p$  interactions is identical in character to that observed in  $pp$  interactions in the same energy region: the data are in good agreement with a logarithmic dependence.<sup>[35]</sup> In the case of  $K^-p$  interactions, the cross sections for producing  $\Lambda$  hyperons fall off with energy in the low-energy region but remain practically constant over the range from 10 to 32 GeV/c. The fall in the cross sections at low energies can be explained by the decreasing contribution from processes involving the annihilation of strangeness in the virtual  $K^+K^-$  scattering in the reaction  $K^-p \rightarrow \Lambda + \text{pions}$ . With increasing energy, other mechanisms for producing  $\Lambda$  hyperons, such as the process  $K^-p \rightarrow \Lambda K \bar{K} + \text{pions}$ , begin to make significant contributions, and this leads to approximately constant cross sections for  $\Lambda$  hyperons in the interval from 10 to 32 GeV/c. On the basis of the trend shown by the data, we might expect that the cross sections for producing  $\Lambda$  hyperons will begin to rise at still higher energies, as in  $K^-p$  interactions.

#### 4. REGULARITIES IN THE APPROACH TO SCALING AND INCLUSIVE DISTRIBUTIONS

Studies of the regularities in the approach to the scaling limit at the phenomenological level are based on the application of the generalized optical theorem,<sup>[36]</sup> which relates the inclusive cross section  $f(p_c, s)$  for the reaction  $ab \rightarrow cX$  to the discontinuity of the six-point amplitude for the process  $ab\bar{c} \rightarrow ab\bar{c}$  in the  $M_X^2$ -channel ( $M_X^2 = (p_a + p_b - p_c)^2$ ), as illustrated schematically in Fig. 5a. The additional hypothesis that the six-point amplitude can be parametrized in a Regge form with the same leading singularities as those used to describe elastic scattering leads to the three limiting cases shown by the

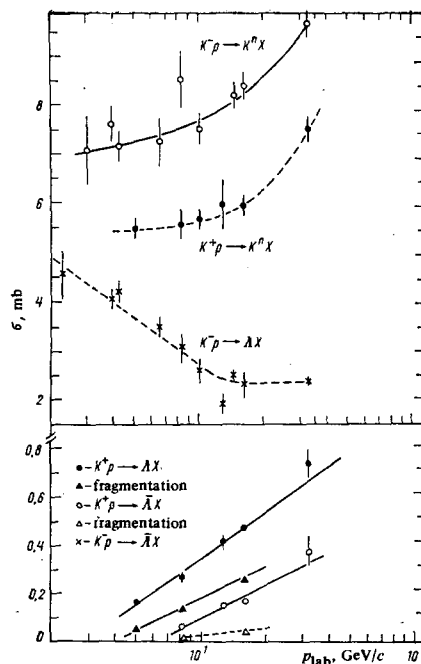


FIG. 4. The  $K^n$ ,  $\Lambda$ , and  $\bar{\Lambda}$  inclusive cross sections as a function of the primary momentum for  $K^+p$  interactions. We also show here the contributions of the fragmentation cross sections for  $\Lambda$  and  $\bar{\Lambda}$  in  $K^+p$  interactions (see Ref. 26).

diagrams b-d of Fig. 5:

a) the fragmentation region (Fig. 5b) of the beam or the target, corresponding to fixed values of  $M^2/s$  and  $t$  with  $s \rightarrow \infty$  and  $M^2 \rightarrow \infty$ ;

b) the triple-reggeon region (Fig. 5c), corresponding to a fixed value of  $t$  with  $s \rightarrow \infty$ ,  $M^2 \rightarrow \infty$ , and  $s/M^2 \gg 1$ ;

c) the central region (Fig. 5d), corresponding to a fixed value of  $y$  in the c. m. s. with  $s \rightarrow \infty$ ,  $t \rightarrow \infty$ , and  $u \rightarrow \infty$  ( $tu \approx sm_T^2$ ).

In the following subsections, we shall carry out a detailed analysis of the regularities in the approach to scaling in the fragmentation and central regions. Owing to the relatively small quantity of new data referring to the triple-reggeon region, we cannot consider this kinematic region, and we limit ourselves to references to recent reviews. [6, 37, 38]

#### a) Approach to the scaling limit in the fragmentation region

The generalized optical theorem and the hypothesis that the leading Regge poles factorize for fixed  $M^2/s$  and  $t$  with  $s \rightarrow \infty$  and  $M^2 \rightarrow \infty$  lead to the following expressions [39] for the fragmentation regions of the particles  $a$  and  $b$ , respectively:

$$\rho \approx \sum_i \beta_i^{ac} \left( \frac{M^2}{s}, p_T \right) s^{\alpha_i(0)-1}, \quad (4.1)$$

$$\rho \approx \sum_j \beta_j^{bc} \left( \frac{M^2}{s}, p_T \right) s^{\alpha_j(0)-1}, \quad (4.2)$$

where  $\rho = f(p_c, s)/\sigma_{tot}$  and  $\alpha_i(0)$  are the intercepts of the appropriate Regge trajectories. Taking the values  $\alpha(0) = 1/2$  for the  $\rho$ ,  $f$ ,  $\omega$ , and  $A_2$  trajectories and  $\alpha(0) = 0$  for the  $f'$  and  $\varphi$  trajectories, the energy dependence of the structure functions  $\rho(M^2/s, p_T^2, s)$ , or equivalently  $\rho(p_{1ab}, p_T^2, s)$ , since fixed values of  $M^2/s$  correspond to fixed values of  $p_{1ab}$  or  $y_{lab}$ , is determined by the expression

$$\rho \left( \frac{M^2}{s}, p_T^2, s \right) = \beta_P \left( \frac{M^2}{s}, p_T^2 \right) + \frac{1}{\sqrt{s}} \sum_{i=f, \rho, \omega, A_2} \beta_i \left( \frac{M^2}{s}, p_T^2 \right) + \frac{1}{s} \sum_{i=f', \varphi} \beta_i \left( \frac{M^2}{s}, p_T^2 \right), \quad (4.3)$$

where  $\beta_P$  is independent of the type of beam (target) particle in the fragmentation region of the target (beam) by virtue of the factorization properties of the Regge-pole amplitudes. The inclusive sum rules (2.6) and (4.3) lead to the following expression for the average multi-

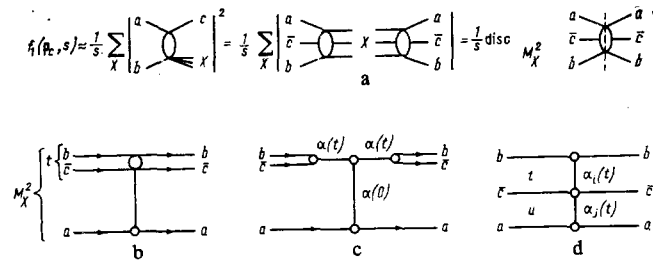


FIG. 5.

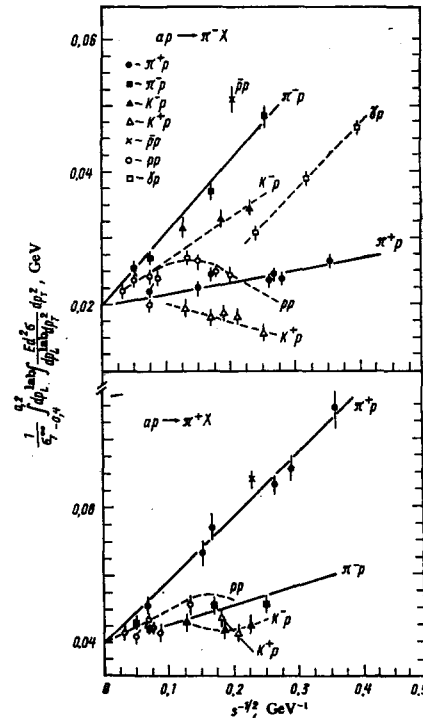


FIG. 6. Approach to scaling in the fragmentation region of the proton for inclusive production of  $\pi^+$  mesons. The points show the data from Ref. 42 and certain additional published data.

licity of particles in the fragmentation region:

$$\langle n \rangle_{fr} \approx A + \frac{B}{\sqrt{s}} + \frac{c}{s}, \quad (4.4)$$

where the last term is due to exchanges involving the  $f'$  or  $\varphi$  trajectory, which are absent in most inclusive reactions.

The experimental regularities in the approach to scaling in the fragmentation region of the target have been widely discussed in the past two years. [6, 7, 40-42] However, the conclusions are highly contradictory, reflecting the statistical unreliability of the data in this kinematic region at the highest energies. In fact, most of the data on the inclusive production of pions obtained using the CERN intersecting storage rings (CERN ISR) correspond to  $p_T > 0.4$  GeV/c or  $y_{lab} > 0$ , while bubble-chamber data are usually integrated with respect to the transverse momenta because of the poor statistics.

The present situation regarding the approach to scaling in the fragmentation of the proton into  $\pi^+$  mesons is illustrated in Fig. 6, in which we present a compilation of data [42] obtained from bubble-chamber experiments. The data at the highest energies indicate that a scaling limit seems to exist, that this limit is generally approached from above, and that factorization holds at the limiting energies. Reactions in which none of the quantum numbers ( $ab$ ,  $ab\bar{c}$ ,  $b\bar{c}$ ,  $a\bar{c}$ ) are exotic<sup>3)</sup> and which do not involve exchanges of the  $f'$ - $\varphi$  trajectory, as, for example, in the reactions  $\pi^+p \rightarrow \pi^+X$ ,  $K^+p \rightarrow \pi^+X$ , or  $\gamma p \rightarrow \pi^+X$ , exhibit a strong energy dependence consistent

<sup>3)</sup> Exotic states are those having quantum numbers which are absent in the usual  $SU(3)$  scheme.

TABLE III. The exotic character of various combinations for the reactions  $ab \rightarrow cX$ .

Reaction	$ab$	$ab\bar{c}$	$a\bar{c}$	$b\bar{c}$
$pp \rightarrow \pi^+ X$	exotic	exotic		
$\pi^+ p \rightarrow \pi^+ X$		exotic	exotic	
$K^+ p \rightarrow \pi^+ X$	exotic	exotic	exotic	
$pp \rightarrow \pi^+ X$	exotic	exotic		
$\pi^+ p \rightarrow \pi^+ X$			exotic	
$K^+ p \rightarrow \pi^+ X$	exotic	exotic		
$K^+ \pi^- \rightarrow \pi^+ X$			exotic	

with the prediction (4.3). Similar reactions in which at least one of the combinations  $ab$ ,  $ab\bar{c}$ , or  $a\bar{c}$  is exotic (Table III) have only a weak energy dependence. From the point of view of the representation (4.3), this is due to a total or partial cancellation between the contributions of the secondary trajectories. Apparently, the growth of the cross sections from threshold observed in the reactions  $pp \rightarrow \pi^+ X$  and  $K^+ p \rightarrow \pi^+ X$  and possibly in the reaction  $K^+ p \rightarrow \pi^+ X$  is due to the fact that the state  $(ab)$  is exotic. It would be of interest to study the relationship between the exotic character of various combinations of particles and the energy dependence of the inclusive cross section for the production of  $\pi^+$  mesons in the fragmentation region of the beam; the reactions  $\pi^+ p \rightarrow \pi^+ X$  and  $K^+ p \rightarrow \pi^+ X$ , in which only the states  $(a\bar{c})$  are exotic, would be of special interest.

The data on the fragmentation of the target into heavy particles at high energies are the most meager. Qualitatively, the character of the approach to the scaling limit in the case of fragmentation of the proton into neutral kaons or  $\Lambda$  hyperons (Fig. 7) is similar to the trend observed for  $\pi^+$  mesons. In particular, factorization is found to be valid in a first approximation, and all the reactions involving the exotic channel  $(ab)$  exhibit a growth of the cross sections from threshold.

An exception is the reaction  $K^+ p \rightarrow K^+ X$ , in which the cross sections are found to fall off sharply with increasing energy as a result of the large contribution from processes involving the annihilation of strangeness in the virtual  $K^+ Y^* \pi^+$  scattering at low energies, where the exchange of the  $f^+ - \psi$  trajectory is dominant.<sup>[43,44]</sup> Consequently, the energy dependence of this reaction in the fragmentation region of the proton (Fig. 8a) is determined by the dominant contribution of the last term in (4.3). On the other hand, the cross sections for pro-

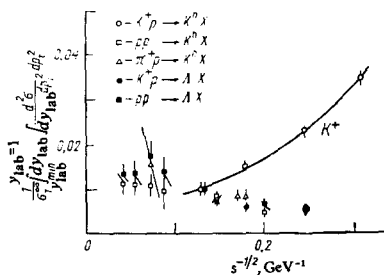


FIG. 7. Approach to scaling in the fragmentation region of the proton for inclusive production of  $K^+$  and  $\Lambda$ . The points are from a compilation<sup>[12]</sup> of published data.

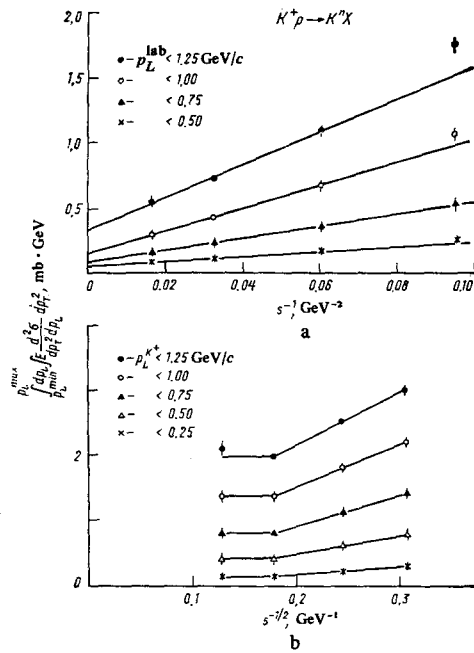


FIG. 8. Energy dependence of the structure functions for the reaction  $K^+ p \rightarrow K^+ X$  in the fragmentation region of the proton (a) (the lines show a "fit" to the data for 8.2–32 GeV/c) and in the fragmentation region of the primary  $K^+$  meson (b) (the lines are drawn by eye through the experimental points) (from Ref. 32).

ducing  $K^+$  mesons in this reaction in the fragmentation region of the beam (Fig. 8b) are determined by the leading contribution of the  $\rho - A_2$  trajectory (the second term in (4.3)) and fall off like  $s^{-1/2}$  in the range of primary momenta from 5 to 16 GeV/c.<sup>[44]</sup> An unexpected energy dependence of the cross sections in the range from 16 to 32 GeV/c<sup>[32]</sup> is illustrated in greater detail in Figs. 9 and 10. In the fragmentation region of the proton, i. e., for small values of  $p_L^{lab}$  (Fig. 9a), the structure function decreases systematically with increasing energy. At the same time, in the fragmentation region of the beam, i. e., for small values of  $p_L^{K^+}$  (where  $p_L^{K^+}$  is the longitudinal momentum of the  $K^+$  meson in the rest system of the primary  $K^+$  meson), the values of the structure functions remain unchanged for primary momenta within the range between 16 and 32 GeV/c (see Fig. 9b). It can be seen from Fig. 10 that within this range of primary momenta the differential cross sections  $d\sigma/d(M^2/s)$  are identical over practically the entire range of the variable  $M^2/s$ , where  $M^2$  is the square of the missing mass.<sup>4)</sup> It seems natural to attribute this surprising behavior to an appreciable growth of the cross sections for pair production of  $K^+ K^+$  mesons over the range of primary momenta from 16 to 32 GeV/c (see Sec. 3). We shall show later that, at least in the central region, the observed precocious scaling in the reaction  $K^+ p \rightarrow K^+ X$  in this energy range is probably fortui-

<sup>4)</sup>The marked energy dependence of the cross section for fragmentation of the proton into  $K^+$  has little effect on the energy dependence of the differential cross section  $d\sigma/d(M^2/s)$  because of the small contribution which the cross section for this process makes to the total inclusive cross section for the reaction  $K^+ p \rightarrow K^+ X$ .

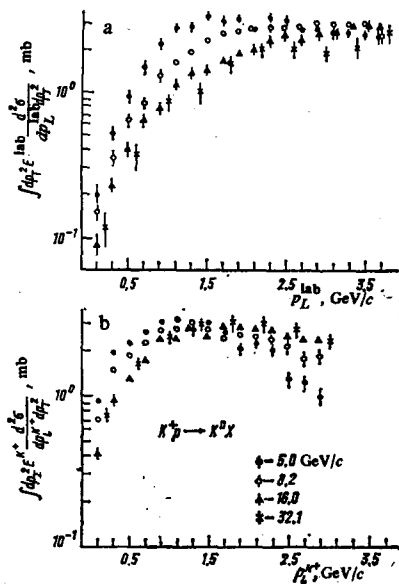


FIG. 9. Invariant distributions for the inclusive reaction  $K^*p \rightarrow K^n X$  as a function of the longitudinal momentum of the  $K^n$  meson in the laboratory system (a) and in the rest system of the primary  $K^*$  meson (b) (from Ref. 32).

tous and that we should expect an appreciable growth of the cross sections for  $K^n$  mesons at still higher energies.

Further evidence for the existence of an asymptotic limit (Fig. 11) comes from the results of an experiment using an electronic detector<sup>[45]</sup> to measure the energy dependences of the yields of  $\pi^+$  mesons in  $p^*p$ ,  $K^*p$ , and  $\pi^*p$  interactions in the fragmentation region of the proton at  $p_T \approx 0.3$  GeV/c and  $y_{lab} \approx 0.6$  over the range of primary momenta from 4 to 250 GeV/c. A characteristic feature of these data is the approach to the scaling limit from below in the case of the reactions  $pp \rightarrow \pi^+ X$ , in contrast with the previously mentioned bubble-chamber data (see Fig. 6), according to which the cross sections for these reactions first rise and then fall as the asymptotic limit is approached. Since the bubble-chamber data correspond to the region  $y_{lab} < 0$  and are integrated over the entire range of transverse momenta, it is difficult to say at the present time whether the results of these experiments are mutually inconsistent, particularly be-

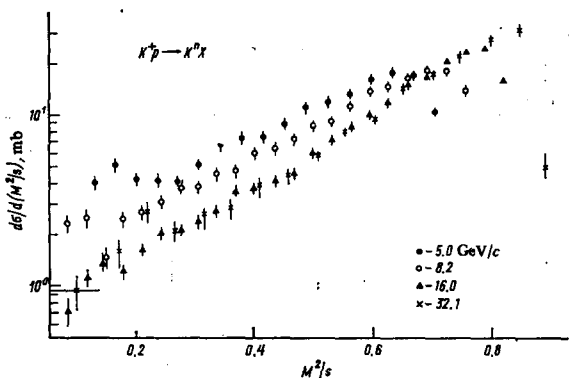


FIG. 10. Differential cross sections  $d^2\sigma/d^2q d(M^2/s)$  for the reaction  $K^*p \rightarrow K^n X$  (from Ref. 32).

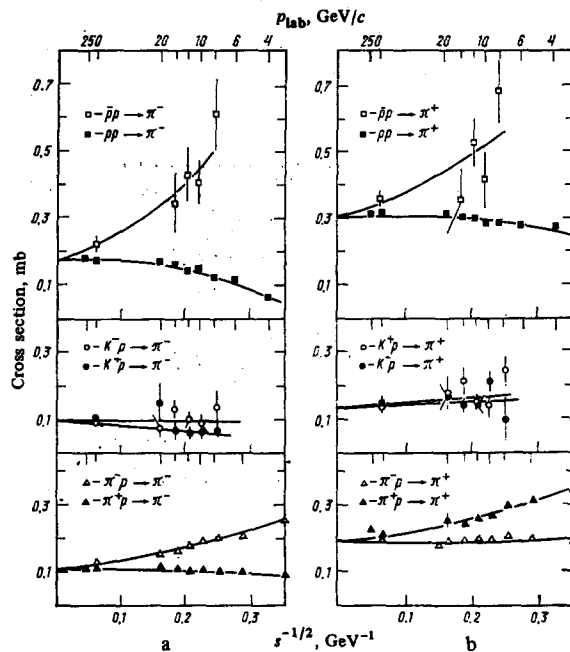


FIG. 11. Energy dependence of the invariant cross sections (integrated over the kinematic region  $0.3 < p_{lab}^* < 0.6$  GeV/c and  $60.75^\circ < \theta_{lab}^* < 64.25^\circ$ ):  $\pi^-$  mesons (a) and  $\pi^+$  mesons (b) in  $p^*p$ ,  $K^*p$ , and  $\pi^*p$  interactions. The curves show fits to the expressions  $A + s^{-1/2}$  or  $A + Bs^{-1/2} + Cs^{-1}$  (from Ref. 46).

cause only two points have been measured at high energies in the electronic experiment. A good fit to the energy dependence of the recent data is given by the expression  $A + Bs^{-1/2} + Cs^{-1}$ . The last term depending on  $s^{-1}$  is of course not due to the contribution of the  $f'$ - $\varphi$  trajectory, as in the case of the reaction  $K^*p \rightarrow K^n X$ , but is evidently due to the higher-order neglected terms in the expansion (4.3). It is clear that much more accurate experimental data in the various regions of phase space would be required to determine the actual  $s$ -dependence of the invariant cross sections in the fragmentation region.

In this connection, it would be of particular interest to measure the energy dependence of the difference between the structure functions for the inclusive reactions  $A^*p \rightarrow cX$  and  $A^-p \rightarrow cX$ . According to (4.3), for reactions which do not involve exchange of the  $f'$ - $\varphi$  trajectory, we have  $f = f(A^*p \rightarrow cX) - f(A^-p \rightarrow cX) = \text{const } s^{-1/2}$ . The few data which permit such a comparison (Fig. 12) suggest

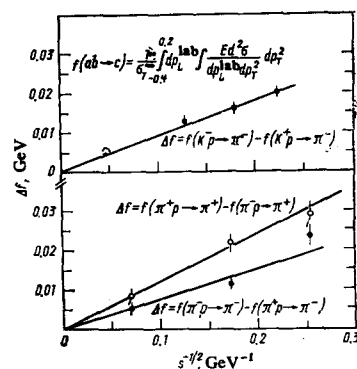


FIG. 12. Energy dependence of the difference between the structure functions.



TABLE IV. Test of factorization of the Pomeranchuk trajectory.

	$f(ap \rightarrow c)/f(a'p \rightarrow c)/s \rightarrow \infty$				Quark model
	$c = \pi^-$	$c = \pi^+$	$c = K^+$	$c = p$	
$\frac{\pi p \rightarrow c}{pp \rightarrow c}$	$0.63 \pm 0.03$	$0.62 \pm 0.03$	$0.25 \pm 0.18$	$0.62 \pm 0.03$	0.67
$\frac{Kp \rightarrow c}{pp \rightarrow c}$	$0.60 \pm 0.06$	$0.45 \pm 0.04$		$0.61 \pm 0.08$	0.67

that this prediction is correct and are consistent with factorization of the leading trajectories.

A test of factorization of the leading Pomeranchuk trajectory which has been made by the Pennsylvania group<sup>[45]</sup> shows that the ratios of the inclusive cross sections for the reactions  $ap \rightarrow cX$  and  $a'p \rightarrow cX$  obtained by extrapolating the energy dependences  $A + Bs^{-1/2} + Cs^{-1}$  (for statistically reliable data) and  $A + Bs^{-1/2}$  (for data with poor statistics) to  $s \rightarrow \infty$  are in reasonable agreement with the ratios of the total cross sections

$$\frac{f(ap \rightarrow c)}{f(a'p \rightarrow c)} \Big|_{s \rightarrow \infty} = \frac{\sigma_{tot}(ap)}{\sigma_{tot}(a'p)}$$

predicted by the additive quark model (Table IV). A similar conclusion was obtained by the SLAC group,<sup>[46]</sup> who measured the ratios  $R$  of the inclusive cross sections for particles and antiparticles in the reactions  $A^*p \rightarrow A^*X$  ( $A = \pi, K, p$ ) at 10 and 14 GeV/c for  $|t| < 0.25$  (GeV/c)<sup>2</sup>.

An integration of  $R$  over the whole accessible range of missing masses  $M$  yields  $R = 0.96 \pm 0.04, 0.90 \pm 0.02,$  and  $1.02 \pm 0.02$  for inelastic  $K^+, \pi^+,$  and  $p^+$  scattering, respectively, at 10.4 GeV/c. These values indicate that the contribution from exchanges with  $C = -1$  is very small in these reactions in comparison with elastic scattering, where this contribution is large at the same energies.

A test of factorization of the leading trajectories in the diffraction processes  $pp \rightarrow pX, pp \rightarrow (p\pi^+\pi^-)X,$  and  $pp \rightarrow (\Lambda K^+)X$  at  $\sqrt{s} = 53$  GeV using the CERN ISR<sup>[47]</sup> showed that this property holds to an accuracy of 5% for  $|t| < 0.5$  (GeV/c)<sup>2</sup>. However, the elastic and inelastic diffraction cross sections for  $|t| > 0.5$  (GeV/c)<sup>2</sup> exhibit an appreciable deviation from factorization, which is evidently due to a large contribution from Regge cuts in this range of  $t$ . This is demonstrated in Fig. 13, where we show the ratios of collinear and non-collinear events as functions of the momentum transfer  $t$  for the three reactions mentioned above. These ratios are related to the differential cross sections as follows:

$$R_p = \frac{\epsilon_p(d\sigma_{el}/dt)}{\epsilon_p((1/2)d\sigma_{SD}/dt)}, \quad R_{p\pi\pi} = \frac{\epsilon_{p\pi\pi}((1/2)d\sigma_{SD}/dt)}{\epsilon_{p\pi\pi}(d\sigma_{DD}/dt)},$$

$$R_{\Lambda K} = \frac{\epsilon_{\Lambda K}((1/2)d\sigma_{SD}/dt)}{\epsilon_{\Lambda K}(d\sigma_{DD}/dt)}.$$

Factorization requires that  $\epsilon_{p\pi\pi} = \epsilon'_{p\pi\pi}$  and  $\epsilon_{\Lambda K} = \epsilon'_{\Lambda K}$ . All three parameters  $R$  are mutually consistent for  $|t| < 0.5$  (GeV/c)<sup>2</sup>, but it is found that the parameter  $R_p$  decreases sharply for  $|t| > 0.5$  (GeV/c)<sup>2</sup>, which indicates that factorization is violated for elastic scattering.

Further evidence for a violation of factorization in the framework of the simple Regge pole model was obtained in Ref. 48, where it was pointed out that the inelastic diffraction and elastic cross sections have different energy dependences:

$$\frac{\sigma(K^-p \rightarrow K^-(n\pi^+); \sqrt{s} = 53 \text{ GeV})}{\sigma(K^-p \rightarrow K^-p; \sqrt{s} = 53 \text{ GeV})} = 7 \pm 1.2\%,$$

$$\frac{1/2\sigma(pp \rightarrow p(n\pi^+); \sqrt{s} = 45 \text{ GeV})}{\sigma(pp \rightarrow pp; \sqrt{s} = 45 \text{ GeV})} = 2.7 \pm 0.7\%.$$

The same conclusion is obtained by comparing the CERN ISR data at  $\sqrt{s} = 45$  GeV with the  $pp$  data at lower energies, where  $\frac{1}{2}\sigma(n\pi^+)_{diff} \approx \sigma_{diff}(p\pi^-) = 0.60 \pm 0.08$  mb, while  $\sigma_{el}(pn) \approx \sigma_{el}(pp) = 8.5 \pm 0.3$  mb for primary momenta equal to 20 GeV/c (for details, see Ref. 48). These results are inconsistent with the predictions of the Regge pole model, according to which the elastic and inelastic diffraction amplitudes should have the same energy dependence  $s^{\alpha_P}$ . The deviation of the parameter  $R$  for elastic scattering in the CERN ISR experiment is evidently due to an appreciable difference between the energy behaviors of the total cross sections.

Thus the energy dependences of the inclusive cross sections in the fragmentation region are consistent with the hypothesis of limiting fragmentation. In this case, the form of the asymptotic spectra in the fragmentation region should be close to that observed at the maximum CERN ISR energies (Fig. 14). It is a remarkable fact that the shape of the rapidity distribution is practically independent of the type of inclusive particle, as shown in Fig. 14b, obtained by simply displacing the spectra of various particles along the rapidity axis and renormalizing them appropriately. Factorization of the leading Regge singularities has been established experimentally for most inclusive reactions with an accuracy of at least 10% for small momentum transfers. However, it is found that there is an appreciable violation of factorization in elastic and inelastic diffraction processes for  $-t > 0.5$  (GeV/c)<sup>2</sup>; this is apparently due to the anomalous behavior of elastic scattering.

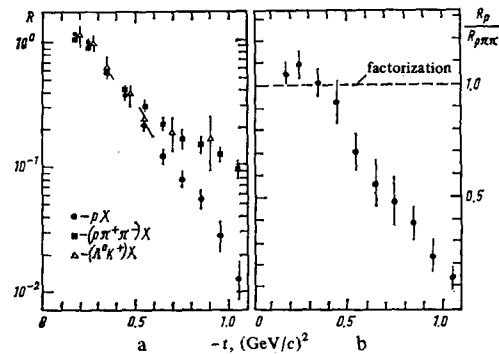


FIG. 13. The ratios  $R_p, R_{p\pi\pi},$  and  $R_{\Lambda K}$  of collinear to non-collinear events (corrected for the loss of non-collinear events) for the reactions  $pp \rightarrow pX, pp \rightarrow (p\pi^+\pi^-)X,$  and  $pp \rightarrow (\Lambda^0 K^+)X$  at  $\sqrt{s} = 53$  GeV (a) and  $R_p/R_{p\pi\pi}$  (b) as a function of the momentum transfer  $t$  (from Ref. 48).

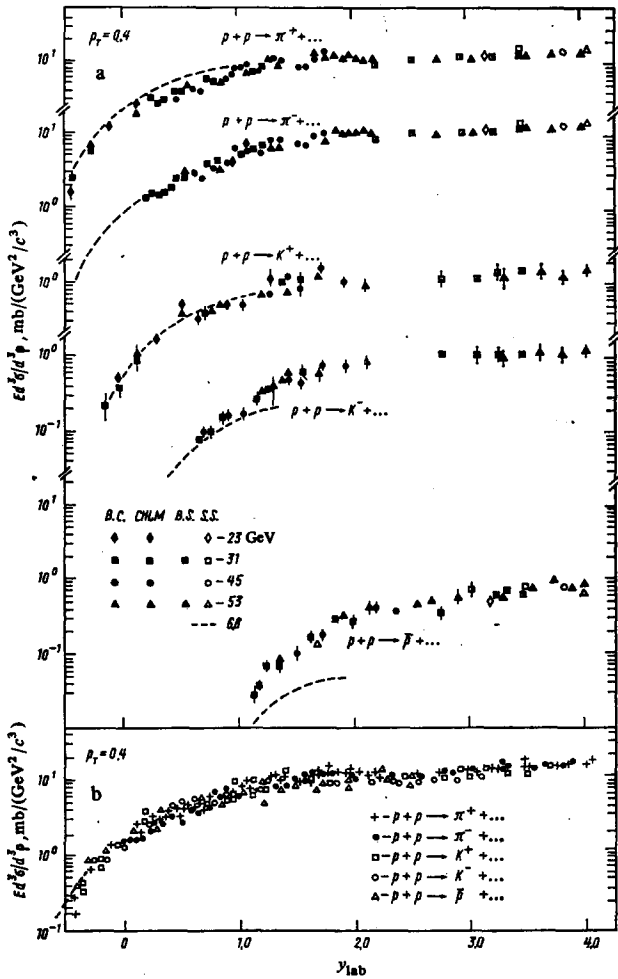


FIG. 14. Invariant rapidity distributions in the laboratory system at  $p_T = 0.4$  GeV/c for  $\pi^+$ ,  $K^+$ , and  $\bar{p}$  in the range of energies  $\sqrt{s}$  from 6.8 to 53 GeV (a), and the same distributions obtained by making a simple displacement in the rapidity and renormalization of the spectra of the various particles (b) (from Ref. 49).

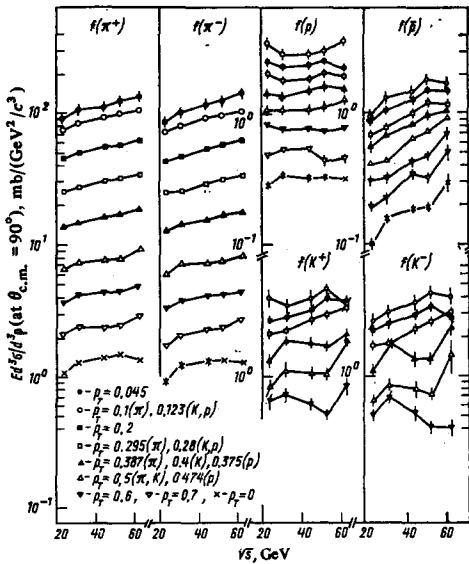


FIG. 15. Energy dependence of the invariant inclusive cross sections for  $\pi^+$ ,  $p^+$ , and  $K^+$  for  $\theta_{c.m.} = 90^\circ$  and various values of  $p_T$  at ISR energies ( $\sqrt{s} = 23, 31, 45,$  and  $63$  GeV) (the data are from Refs. 50–52).

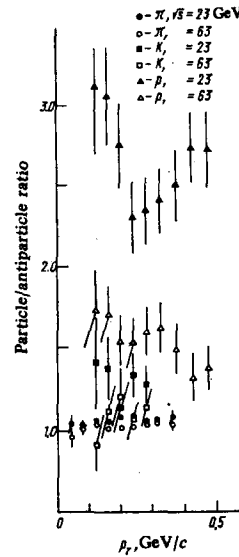


FIG. 16. Ratio of the particle to antiparticle yields as a function of  $p_T$  at  $\sqrt{s} = 23$  and  $63$  GeV (from Ref. 51).

### b) Approach to scaling in the central region

Several important experiments that have recently been carried out using the Serpukhov, FNAL, and CERN ISR accelerators have greatly clarified the character of the energy dependence of the inclusive cross sections in the central region. At the Tbilisi conference, for example, the British-Scandinavian-MIT Collaboration<sup>[50,51]</sup> reported the results of measurements of the inclusive yields of  $\pi^+$ ,  $K^+$ , and  $p^+$  at  $x=0$  in the CERN ISR energy range  $23 \leq \sqrt{s} \leq 63$  GeV for small values of  $p_T$ :  $0.04 \leq p_T \leq 0.4$  GeV/c for  $\pi^+$ ,  $0.1 \leq p_T \leq 0.3$  GeV/c for  $K^+$ , and  $0.1 \leq p_T \leq 0.5$  GeV/c for  $p^+$ . A compilation of these data, together with earlier data at large values of  $p_T$ ,<sup>[52]</sup> is shown in Fig. 15. We see that the scaling limit has not yet been reached, even at the CERN ISR energies. The average growths of the differential cross sections over the ISR energy range from  $\sqrt{s} = 23$  GeV to  $\sqrt{s} = 63$  GeV in the kinematic region under consideration are as follows:

$$\begin{aligned}
 &36 \pm 2\% \text{ and } 41 \pm 2\% \text{ for } \pi^+ \text{ and } \pi^-; \\
 &52 \pm 8\% \text{ and } 69 \pm 8\% \text{ for } K^+ \text{ and } K^-; \\
 &8 \pm 5\% \text{ and } 84 \pm 6\% \text{ for } p \text{ and } \bar{p}.
 \end{aligned}$$

The flux of particles at small  $p_T$  is determined mainly by the yield of pions, but the proportion of heavier particles—kaons and nucleons—rises almost linearly with  $p_T$ . However, the cross sections for pions rise at the minimum values of  $p_T$ . It seems reasonable to attribute this effect to an enhancement in the cross sections for producing resonances, which lead to a large number of pions from the decays of resonances at small values of  $p_T$ . The ratio of the particle and antiparticle yields (Fig. 16) has a strong dependence on  $p_T$  and  $s$  in the case of protons and antiprotons. At the lowest energies and small  $p_T$  an appreciable fraction of the protons at  $x=0$  are actually produced as a result of the fragmentation of the primary particles, although the ratio of the  $p$  and  $\bar{p}$  yields tends to 1 with increasing  $p_T$  and  $s$ , as we should expect for central collisions.

The inclusive distributions of pions with respect to the

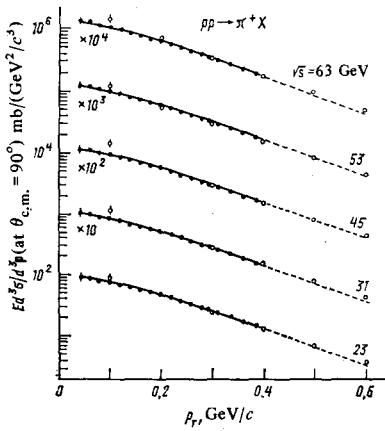


FIG. 17. Invariant  $p_T$  distribution of  $\pi^+$  mesons in the reaction  $pp \rightarrow \pi^+ X$  at  $\theta_{c.m.} = 90^\circ$  and  $\sqrt{s} = 23-63$  GeV (from Ref. 50).

transverse momenta at energies in the range  $\sqrt{s} = 23-63$  GeV<sup>[50]</sup> (Fig. 17) are best described by the parametrization  $\exp(-Bm_T)$  with  $m_T = \sqrt{m_c^2 + p_T^2}$ , which also works well at lower energies.<sup>[53,54]</sup> The indices  $B$  for the exponential slopes of the pion and kaon spectra listed in Table V for energies in the range  $\sqrt{s} = 23-63$  GeV have somewhat higher values for pions than for kaons and are characterized by a weak growth with energy.

The observed strong violation of (Feynman) scaling at  $x=0$  is not surprising and is predicted by many theoretical models.<sup>[55-57]</sup> For example, according to the model of Cheng and Wu,<sup>[55]</sup> the cross section at fixed rapidity in the c. m. s. rises like a power of the energy:

$$\int f(y, p_T^2, s) dp_T^2 \sim A s^{c(1+2c)} \ln s^{2c/(1+2c)}, \quad (4.5)$$

where the parameter  $c = 0.083$  is determined by the energy dependence of the total cross sections.<sup>5)</sup> Logunov *et al.*,<sup>[56]</sup> predict a power growth of the second moment in the multiplicity in the same kinematic region. Regge models<sup>[57]</sup> lead to such a growth of the cross sections if it is assumed that the leading vacuum singularity has an intercept  $\alpha(0) > 1$ .

However, it is possible that the growth of the cross sections in the central region predicted by these models will be important only at much higher energies and that the observed effect is due to a simple falling-off of the contributions from the secondary trajectories in the ordinary double-reggeon representation<sup>[59]</sup>:

$$f(p_c, s) \approx \frac{1}{s} \sum_{i,j} \Phi_{ij}(m_T) |t|^{\alpha_i(0)} |u|^{\alpha_j(0)}, \quad (4.6)$$

where  $\alpha_i(0)$  are the intercepts of the leading trajectories,  $t = (p_a - p_c)^2$ , and  $u = (p_b - p_c)^2$ . In the region of small transverse momenta and fixed rapidities,  $|t| \approx \sqrt{s} m_T e^{-y}$  and  $|u| \approx \sqrt{s} m_T e^y$  are relatively small even in the CERN ISR energy range, so that the contribution from the secondary pole terms is hardly noticeable at these energies. A cancellation of the cut contributions in this kin-

<sup>5)</sup>The energy sum rules (2.9) limit the domain of applicability of (4.5) to the interval  $|y| < \frac{1}{2} \ln(s/s_0)(1 - \Delta)$ ,<sup>[58]</sup> where  $\Delta = c/(1+2c)$ .

matic region, pointed out by Abramovskii, Gribov, and Kancheli<sup>[60]</sup> for asymptotic energies, provides some justification for applying (4.6) with no further correction terms.

Using Eq. (4.6) and the coupling constants  $\delta_R^{a(b)}$  for the reggeon  $R$  and particle  $a(b)$ , which are known from the analysis of the total cross sections, the ratio of the inclusive cross section for the reaction  $a + b \rightarrow c + X$  in the central region and the total asymptotic cross section  $\sigma_{tot}^{ab}(\infty)$  can be written in the form

$$\begin{aligned} \rho(p_c, s) &= \frac{f(p_c, s)}{\sigma_{tot}^{ab}(\infty)} \\ &= \Phi_{PP}(m_T) + s^{-1/4} \left( \sum_R \frac{\delta_R^a}{\delta_P^a} \Phi_{RP}(m_T) e^{y/2} + \sum_R \frac{\delta_R^b}{\delta_P^b} \Phi_{PR}(m_T) e^{-y/2} \right) \\ &\quad + s^{-1/2} \sum_{R,R'} \frac{\delta_R^a \delta_{R'}^b}{\delta_P^a \delta_P^b} \Phi_{RR}(m_T); \end{aligned}$$

here  $\Phi_{ij}(m_T)$  are the double-reggeon vertex functions, which are independent of the type of primary particles and depend only on the type of inclusive particle. The vertex functions  $\Phi_{ij}(m_T)$  are real, but their signs are in general arbitrary.<sup>[59]</sup> General arguments require that  $\Phi_{PP}(m_T)$  is positive. The vertices  $\Phi_{ij}(m_T)$  with  $i, j = \omega, \rho$  change sign on making the substitution  $c \rightarrow \bar{c}$ ; terms in which  $\rho$  or  $\omega$  join a given vertex change sign on making the substitution  $a \rightarrow \bar{a}$  ( $b \rightarrow \bar{b}$ ). However, the absolute phases of the vertices can be fixed only from experiment, as in the case of two-particle reactions. The coupling constants  $\delta_R^{a(b)}$  are normalized as follows:

$$\delta_{tot}^{(ab)}(s) = \delta_P^a \delta_P^b + s^{-1/2} \sum_R \tau_R \delta_R^a \delta_R^b,$$

where  $\tau_R$  is the signature factor.

Equation (4.7) leads to the following interesting consequences<sup>[59]</sup>:

a) there exists an asymptotic plateau in rapidity, whose height  $\Phi_{PP}(m_T)$  is independent of the type of colliding particles and is the same for a particle  $c$  and its antiparticle  $\bar{c}$ ;

b) the energy dependence of the inclusive cross section at fixed  $m_T$  and  $y$  is determined by the expression

$$\rho(y, m_T, s) = \Phi_{PP}(m_T) + \alpha(y, m_T) s^{-1/4} + \beta(y, m_T) s^{-1/2}, \quad (4.8)$$

and the dependence of the inclusive cross section on  $s$  and  $y$  is correlated, in accordance with (4.7);

c) in the energy dependence of the average multiplicity of particles of type  $c$  in the central region,

$$\langle n_c \rangle_{\text{central}} = A_c + B_c \ln s + \frac{D_c}{\sqrt{s}} + \frac{F_c \ln s}{\sqrt{s}}, \quad (4.9)$$

the value of the coefficient of  $\ln s$  is determined by the asymptotic limit for the function  $\rho$ :

TABLE V.

Particle	$\pi^+$	$\pi^-$	$K^+$	$K^-$
$B, \text{GeV}^{-1}$	7.4	7.2	6.6	7.09

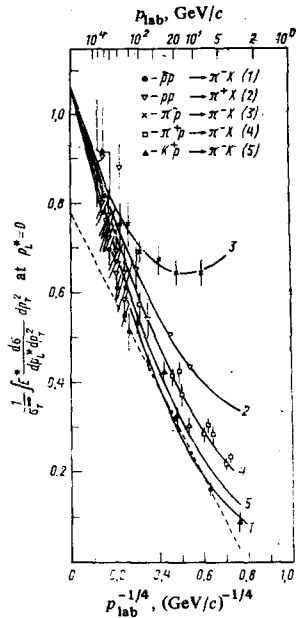


FIG. 18. Energy dependence of the invariant inclusive cross sections for  $\pi^\pm$  mesons in the central region. The points are from a compilation of published data<sup>[12]</sup>; the curves show the result of a double-reggeon fit<sup>[61]</sup> in the space of the variables ( $s, m_T, y$ ) to the data on the reactions  $pp \rightarrow \pi^\pm X$  at 12 and 24 GeV/c.<sup>[53]</sup>

$$B_c = \pi \int d m_T^2 \Phi_{PP}(m_T). \quad (4.10)$$

It was shown in Refs. 54 and 61–63 that this approach actually describes the energy dependences of the inclusive cross sections and the shapes of the rapidity distributions in the central region for many inclusive reactions. An important result is that the vertex functions  $\Phi_{RR}, \Phi_{RP},$  and  $\Phi_{PP}$  have values of the same order of magnitude. In using data at low energies to describe the energy dependence of inclusive cross sections in the central region, we can therefore not neglect the last term in (4.7). The dependences of the vertex functions on  $m_T$  obtained in Ref. 61 from an analysis of the reactions  $pp \rightarrow \pi^\pm X$  at 12 and 24 GeV/c are close to an exponential behavior. The slope parameters  $b_{ij}$  in the parametrization  $\Phi_{ij} = A_{ij} \exp(-b_{ij} m_T)$  are found to be practically identical in the reactions  $pp \rightarrow \pi X, \pi p \rightarrow \pi X,$  and  $Kp \rightarrow \pi X$ .<sup>[61]</sup> Moreover, by comparing the slope parameters in these reactions and in the reaction  $K^*p \rightarrow K^0 X$ , it was found<sup>[54]</sup> that they are also independent of the type of inclusive particle, i. e., they are the same for pions and kaons. This universality in the dependence of the vertex functions on  $m_T$ , which was also pointed out in Ref. 64, is of great interest and will be analyzed in further detail in Sec. 4c.

Let us now consider the regularities in the energy dependences of the invariant inclusive cross sections from the point of view of the representation (4.7). In Figs. 18 and 19 we show a compilation<sup>[12]</sup> of data on the inclusive yields of  $\pi^\pm$  and  $K_S^0$  mesons at high energies (integrated with respect to  $p_T^2$ ) at  $x=0$ . The present situation differs markedly from what was expected several years ago<sup>[66]</sup> (the dashed curves in Figs. 18 and 19 with  $B_r = 0.78$  and  $B_\pi \approx 0.1 B_r = 0.078$ ). The scaling limit has obviously not been reached, even at the highest attainable energies, although the data are consistent with the existence of such a limit which is independent of the type of colliding particles.

The double-reggeon formalism reproduces the trend

of the data up to the maximum energies. The curves 1 and 2 in Fig. 18 show the result of a fit<sup>[61]</sup> of Eq. (4.7) to the data on the reaction  $pp \rightarrow \pi^\pm X$  at 12 and 24 GeV/c in the space of the variables ( $s, m_T, y$ ). The curves 4 and 5 for the reactions  $\pi^+ p \rightarrow \pi^\pm X$  and  $K^+ p \rightarrow \pi^\pm X$  are obtained using the same fit to the data on the reactions  $pp \rightarrow \pi^\pm X$  and the known coupling constants  $\delta_i^{K^+}$  and  $\delta_i^{K^0}$ , taken from the analysis of the total cross sections. It is important to note that the double-reggeon analysis at these relatively low energies generally ensures a fit to the data over a wide range of energies.

In the reaction  $\pi^+ p \rightarrow \pi^\pm X$ , in which there is a strong effect due to the leading particle, the energy dependence of the cross section at low energies is initially noticeably different from that of the other reactions. With increasing energy, however, the same trend is observed. Moreover, a good fit to the energy dependence of the cross section for this reaction is obtained from Eq. (4.7) when the value of  $B_c$  is fixed at the value of  $B_c$  for the reactions  $pp \rightarrow \pi^\pm X$  (the curve 3 in Fig. 18).

The energy dependence of the cross section for the reaction  $pp \rightarrow K_S^0 X$  is again in agreement with the double-reggeon representation (Fig. 19). The double-reggeon parametrization also provides a good fit to the spectra of  $K_S^0$  mesons with respect to the rapidities in the c. m. s. With certain reservations, we can say the same thing about the reaction  $K^*p \rightarrow K_S^0 X$  (Fig. 19), where the RR term in Eq. (4.7) is responsible for the falling-off of the cross section over the range of primary momenta from 5 to 16 GeV/c.<sup>[54]</sup> The cross sections develop a plateau in the interval from 16 to 32 GeV/c, and a double-reggeon fit to the data between 5 and 32 GeV/c made by the France-USSR and CERN-USSR Collaborations<sup>[32]</sup> indicates that the cross sections should begin to rise at high energies. The value  $B_K = 0.152 \pm 0.030$  obtained for this reaction from the fit to the data between 5 and 32 GeV/c in the space of the variables ( $s, m_T, y$ )<sup>[32]</sup> is completely consistent with the asymptotic value for the reaction  $pp \rightarrow K_S^0 X$  (see Fig. 19). Therefore  $K_S^0$  production in the central region is also consistent with factorization.

Thus a growth of the cross sections in the central region at high energies is predicted even for reactions

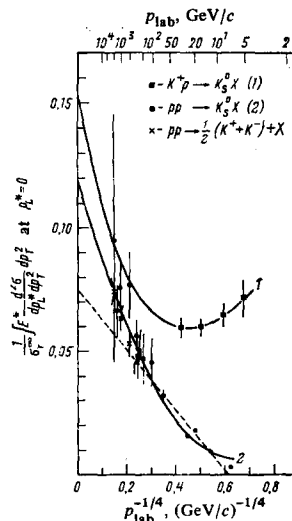


FIG. 19. Energy dependence of the invariant inclusive cross sections for  $K_S^0$  mesons in  $pp$  and  $K^*p$  interactions in the central region. The points are from a compilation of published data.<sup>[12]</sup>

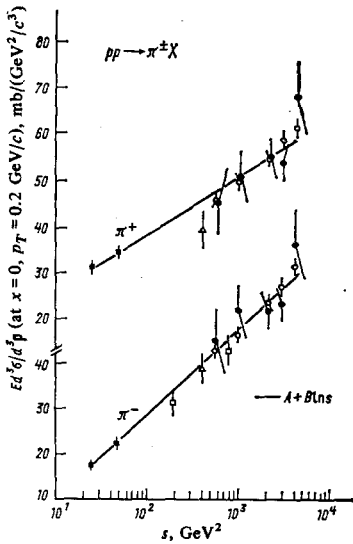


FIG. 20. Energy dependence of the invariant cross sections for the reactions  $pp \rightarrow \pi^\pm X$  at  $x=0$  and  $p_T=0.2$  GeV/c (from Ref. 50).

with a strong leading-particle effect, as can be seen from the double-reggeon analysis of the reaction  $K^+p \rightarrow K^0 X$ , for which the cross section is still decreasing as a function of  $s$  in the accessible energy range, and the reaction  $\pi^+p \rightarrow \pi^+ X$ , for which this growth has been confirmed experimentally, thus refuting the myth of "precocious" scaling in this reaction.

We see that the asymptotic value of the function  $\rho$  determines the value (4.10) of the coefficient  $B_c$  in the energy dependence (4.9) of the average multiplicity of particles of type  $c$  in the central region, and allowance for the contribution to  $\langle n_c \rangle$  from the fragmentation component (4.4) cannot change the value of  $B_c$ . Therefore the double-reggeon representation predicts that the value of the coefficient  $B_{ch}$  of  $\ln s$  in the energy dependence of the average multiplicity of charged particles

$$\langle n_{ch} \rangle = A_{ch} + B_{ch} \ln s + \frac{C_{ch}}{\sqrt{s}} + \frac{D_{ch} \ln s}{\sqrt{s}} \quad (4.11)$$

is determined by the sum of the coefficients  $B_c$  for all charged particles. Neglecting the contributions from particles heavier than kaons and using the values  $B_\pi = B_\rho \approx 1.05$  and  $B_{K^+} = B_{K^-} \approx 0.12$  (see Figs. 18 and 19), we have

$$B_{ch} \approx 2B_\pi + 2B_K \approx 2.34. \quad (4.12)$$

In this connection, it is of interest to note that fits to the experimental  $s$ -dependences of  $\langle n_{ch} \rangle$  for  $pp$ ,  $\pi p$ , and  $Kp$  interactions using Eq. (4.11) and assuming that  $B_{ch}$  should have the same value for different types of interactions lead to the value  $B_{ch} = 2.35 \pm 0.18$ ,<sup>[67]</sup> in good agreement with (4.12) and appreciably larger than the result obtained from the usual "logarithmic" fits using only the first two terms in (4.11). It is therefore necessary to exercise care in comparing the multiplicities of secondary particles in cosmic rays at energies  $10^{12}$ – $10^{16}$  eV with extrapolations of data at accelerator energies.

However, an analysis of data obtained from extensive atmospheric showers also suggests an even greater increase in the multiplicities of secondary particles at cosmic-ray energies.<sup>[68]</sup> Other cosmic-ray data<sup>[69–71]</sup> presented at the Tbilisi conference also indicate a deviation from scaling (for details, see Ref. 72). Of course, this evidence is not surprising, since a strong violation of scaling already occurs at accelerator energies. What is important is a degree of violation of scaling that may be consistent with either asymptotically energy-independent cross sections or cross sections which rise indefinitely.

We might conclude from the foregoing discussion that the data are compatible with the existence of the asymptotic limit predicted by the double-reggeon approach. However, this conclusion would probably be premature. The compilation of data given by the British-Scandinavian-MIT Collaboration<sup>[50]</sup> serves as a warning against a possible bias. The invariant cross sections for the reactions  $pp \rightarrow \pi^\pm X$  at  $x=0$  and  $p_T=0.2$  GeV/c, shown in Fig. 20 as a function of  $\ln s$ , are indeed in agreement with the predictions of the double-reggeon formalism, but are also compatible with a logarithmic or even a power growth of the cross sections ( $A + Bs^\alpha$  with  $\alpha > 0$ ), i. e., with the absence of a scaling limit.

In this connection, it is of some interest to ask what to do about the predictions of an asymptotic unlimited growth of the cross sections in the central region, which we mentioned at the beginning of this subsection. We are concerned here with possible mechanisms which lead to the maximal growth of the cross sections in models with  $s$ -channel unitarization,<sup>[55]</sup> which predict a power growth of the cross sections of the type (4.5) at fixed rapidities in the c. m. s., or with theoretical ideas<sup>[56]</sup> according to which the energy growth of the second moment in the multiplicity  $\langle n_c n_d \rangle$  in the pionization region of the inclusive reaction  $ab \rightarrow cdX$  can be very large,  $\lesssim s/\ln^\alpha s$  ( $\alpha > 0$ ), under certain conditions on the choice of phase space. Studies of the associated multiplicities  $\langle n(M_X^2) \rangle$  for a number of inclusive reactions  $ab \rightarrow cX_d$  have shown, for example, that they are characterized by different dependences on  $M_X^2$  in the fragmentation and central regions, the growth with  $M_X^2$  being more rapid in the central region.<sup>[73–75]</sup> It seems to us that this situation is very reminiscent of the status of the energy dependence of the total cross sections prior to the discovery of the Serpukhov effect. We recall that the Regge pole model predicted that the cross section should tend to a constant according to the law  $a + b/\sqrt{s}$ . The deviation from this simple dependence observed in experiments using the Serpukhov accelerator led to important changes in our ideas about the nature of particle interactions at high energies. It is therefore tempting to analyze the energy dependences of the experimental cross sections for inclusive processes in the central region to ascertain whether they deviate appreciably from the predictions of the double-reggeon formalism. In view of the constant improvement in the accuracy of the experimental data, there is every reason to expect that such an analysis might become possible in the near future.

At what energies should we expect appreciable deviations from the predictions of the double-reggeon approximation? We recall (see Sec. 2) that the scaling parameter which determines the threshold energy for the new mechanism leading to a growth of the total cross sections with maximum saturation of the partial waves in (2.14) is  $s_0 \approx 120 \text{ GeV}^2$ . The cross section for an inclusive process in the central region is related to the discontinuity of the six-point amplitude in the  $M_X^2$ -channel (see the graphs a and d in Fig. 5), and the square of the total energy in the channel  $a\bar{c}$  or  $b\bar{c}$  is  $\sqrt{s} \langle m_T \rangle$ , i. e.,  $\approx 60 \text{ GeV}^2$  even at the highest CERN ISR energies. It is therefore possible that new effects analogous to the growth of the total cross sections will appear only at energies much higher than those which are accessible using existing accelerators. An analysis of the passage of secondary particles from cosmic rays through the atmosphere suggests that this may happen at energies of  $10^{14} - 10^{16} \text{ eV}$ . However, we note that these considerations involve the implicit assumption that there is a universal scale for  $s$  of the order of  $1 \text{ GeV}$ . But there are good reasons to suppose (see the preceding sections) that the energy scale in the inclusive spectra of particles is given by the average value  $\langle m_T \rangle$  of the transverse mass. In this case, deviations from the Regge pole approximation may appear at lower energies. Clearly, a quantitative analysis of these interesting phenomena will have to await a new generation of accelerators with intersecting rings and energies  $\approx 2 \text{ TeV}$ .

### c) Transverse scaling

In discussing the double-reggeon representation, we have already pointed out that the vertex functions  $\Phi_{ij}(m_T)$  depend exponentially on the transverse mass  $m_T$  and that the parameters of the exponential slopes are universal, i. e., they are independent of both the type of colliding particles and the type of inclusive particle. This interesting circumstance can be explained in a natural way<sup>[65]</sup> in the framework of the multiperipheral model, in which the appropriate vertices  $\Phi_{ij}(m_T)$  originate from a summation of ladder diagrams. Adopting the usual exponential cut-off ( $e^{bt}$ ) in each rung of the multiperipheral diagram, the vertex functions can be represented in the form

$$\Phi_{ij}(m_T) = \text{const} \cdot g^{[\alpha_i(0) - \alpha_j(0)]/2} e^{-g\Psi(\alpha_j(0) + 1, \alpha_j(0) - \alpha_i(0) + 1, g)}, \quad (4.13)$$

where  $g = bm_T^2$  and  $\Psi$  is the hypergeometric function. The only free parameter (apart from the overall normalization of each of the vertex functions  $\Phi_{ij}$ ) is then the coefficient  $b$ , which determines the universal dependence of  $\Phi_{ij}$  on  $m_T$ . It is found<sup>[65]</sup> that for  $b = 2.05$  the expression (4.13) accurately reproduces the vertex functions determined from fits of (4.7) to the experimental data. The multiperipheral model also accurately reproduces the small difference between the parameters of the exponential slopes for  $\Phi_{PP}$ ,  $\Phi_{PR}$ , and  $\Phi_{RR}$ , which, in the double-reggeon representation, leads to an average transverse momentum  $\langle p_T \rangle$  of the inclusive particle that depends on  $s$  and on the rapidity  $y$ :  $\langle p_T \rangle$  falls off with increasing  $y$  and rises with increasing  $s$ , reaching a maximum value determined by the value of  $\Phi_{PP}(m_T)$ .

If  $m_T \geq 0.4 \text{ GeV}$ , the vertex functions (4.13) are not very different from the asymptotic expression (for large  $m_T$ )

$$\Phi_{ij}(m_T) \approx \text{const} \cdot e^{-bm_T^2 m_T^{-[\alpha_i(0) + \alpha_j(0) + 2]}}$$

and the inclusive cross section can be written in the form

$$\frac{d^2\sigma}{dm_T^2 dy} \approx -\frac{e^{-bm_T^2}}{m_T^2} (1 + \beta_1 \sqrt{ze^y} + \beta_2 \sqrt{ze^{-y}} + \beta_1 \beta_2 z), \quad (4.14)$$

where  $z = m_T/\sqrt{s}$ . Thus, if  $m_T \geq 0.4 \text{ GeV}$ , the energy-dependent part of the inclusive cross section can be represented in the scaling form (4.14) with respect to the transverse mass  $m_T$ , and the scaling law of the type  $\Phi(p_T)F(p_T/\sqrt{s})$  which is observed for  $y=0$  and  $p_T > 2 \text{ GeV}/c$  (so-called transverse scaling) is valid down to small values of  $p_T$  and  $s$ , but with the change of variable  $p_T/\sqrt{s} \rightarrow m_T/\sqrt{s}$ . It follows from (4.14) that for  $y \neq 0$  the inclusive cross section can be written in the factorized form

$$\frac{d^2\sigma}{dm_T^2 dy} \sim \Phi(m_T) \Psi_1(x_1) \Psi_2(x_2), \quad (4.15)$$

where

$$x_1 = ze^y = \frac{E + p_T}{\sqrt{s}} \quad \text{and} \quad x_2 = ze^{-y} = \frac{E - p_T}{\sqrt{s}} \quad (4.16)$$

are the light-cone variables. We see that the inclusive cross section in the central region (like the cross section in the fragmentation region; see Sec. 4d) can be represented in a factorized form in the variables  $m_T$ ,  $x_1$ , and  $x_2$ .

The universality of the inclusive distributions in  $m_T$  can be used to estimate the yields of heavy particles from the known cross sections for producing light particles with large  $p_T$ . At  $y=0$ , the spectra of pions with large  $p_T$  are well approximated by the expression<sup>[78]</sup>

$$f(y=0, p_T^2, s) \approx Am_T^{-N} e^{-Bm_T/\sqrt{s}}$$

with  $N \approx 8$  and  $B \approx 26$ . Assuming that only the overall normalization changes in the case of heavier particles, reasonable estimates are obtained<sup>[77]</sup> for the cross sections for producing  $\rho$ ,  $\omega$ ,  $\varphi$ , and  $J$  mesons, in agreement with experiment, and for the yields of charmed particles.

### d) Relation to deep inelastic scattering

An interesting approach to the behavior of the inclusive cross sections in the fragmentation region was proposed by Logunov *et al.*<sup>[78]</sup> Using the Jost-Lehmann-Dyson representation for the spectral functions, they showed that the inclusive cross section in the region of large values of the variable  $\gamma = 2p_b(p_a + p_c)/2p_b(p_a - p_c)$  can be written in the form

$$f(p_c, s) = \gamma^{\alpha(q^2, v)} F(q^2, v), \quad (4.17)$$

where

$$q^2 = (p_a - p_c)^2, \quad v = 2p_b(p_a - p_c).$$

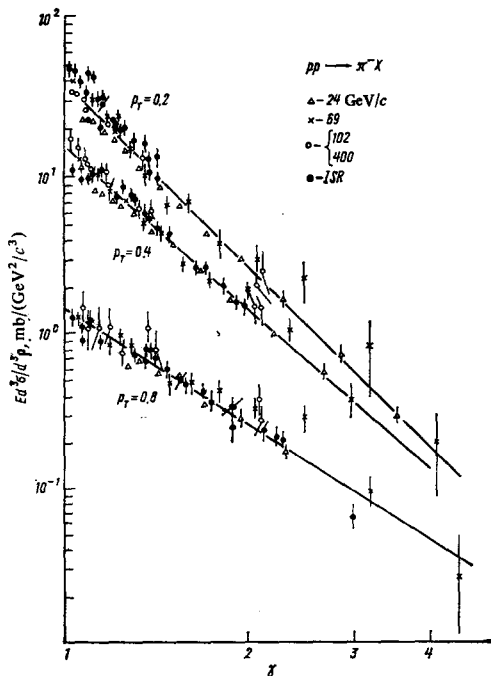


FIG. 21. Inclusive cross sections for the reaction  $pp \rightarrow \pi^- X$  as a function of the variable  $\gamma$  (the straight lines are drawn by eye (from Ref. 79)).

If the spectral function has no singularities, then  $a(q^2, \nu) < 0$ ; otherwise, we have  $a(q^2, \nu) > 0$ . It can be seen from Fig. 21<sup>[79]</sup> that the representation (4.17) fits the data with a weak dependence of  $a(q^2, \nu)$  and  $F(q^2, \nu)$  on  $\nu$ . It is found that  $a(q^2, \nu) < 0$  for the reactions  $pp \rightarrow \pi^+ X$ , while  $a(q^2, \nu) > 0$  for the reactions  $pp \rightarrow p X$ <sup>[79]</sup> and  $K^+ p \rightarrow K^0 X$ <sup>[80]</sup> with strong leading-particle effects. Thus it seems possible to associate leading-particle effects with singularities in the Jost-Lehmann-Dyson spectral function.

At  $p_T = 0.4$  GeV/c, i. e., at a transverse momentum near the average transverse momentum of the pions in  $pp$  collisions, we have  $a(q^2, \nu) \approx 3$ . Since  $\gamma \approx (1+x)/(1-x)$  for large  $\gamma$ , this behavior corresponds to an inclusive cross section which falls off as  $x \rightarrow 1$  according to the law  $f \sim (1-x)^3$ . As pointed out in Ref. 81, such a behavior of the pion spectrum in  $pp$  interactions is to some extent in conflict with the triple-reggeon approximation, but it is in agreement with the simple quark-parton picture of the interaction if it is assumed that the pion spectrum in the region of large  $x$  reproduces the behavior  $\nu W_2(x) \sim (1-x)^3$  of the proton structure function. Moreover, it is found<sup>[79]</sup> that the invariant cross section factorizes in the variables  $\gamma_a$  and  $\gamma_b$  referring to the fragmentation of the beam and target, respectively, and has the form

$$f \approx \Phi(m_T) \Psi_a(\gamma_a, m_T) \Psi_b(\gamma_b, m_T). \quad (4.18)$$

The functions  $\Psi(\gamma, m_T)$  behave like  $\gamma^{\alpha(m_T)}$  for large  $\gamma$ . Rewriting Eq. (4.18) in terms of the variables  $m_T$ ,  $y$ , and  $s$ , we obtain

$$f \approx \Phi(m_T) \Psi_a\left(\frac{m_T e^y}{\sqrt{s}, m_T}\right) \Psi_b\left(\frac{m_T e^{-y}}{\sqrt{s}, m_T}\right) \quad (4.19)$$

in analogy with Eq. (4.15) for the central region, which follows from the double-reggeon representation of the multiperipheral model<sup>[82]</sup> and certain heuristic arguments put forward by Kinoshita.<sup>[83]</sup>

Equations of the type (4.18) and (4.19), which reflect our ideas about factorization of the forward and backward cones in the inclusive spectra, are also remarkable in that they satisfy "transverse" scaling. These expressions depend on the variables  $m_T$  and  $\sqrt{s}$  through the variable  $m_T/\sqrt{s}$ . This means that the scale of energies is given by the transverse mass and accounts for the slower approach to the asymptotic regime for heavy particles. Finally, as we have already pointed out, the behavior of the functions  $\Psi(z)$  reproduces the behavior of the proton structure function (for large values of  $y$ , we have  $z = m_T e^y/\sqrt{s} - x$ ).

In Ref. 84 an attempt was made to establish a direct relation between the structure function for the deep inelastic scattering process  $ep \rightarrow eX$  and the inclusive cross section for the reaction  $K^+ p \rightarrow K^0 X$ , which is dominated by exchange of the  $\rho$  trajectory. In Fig. 22 we compare the structure function for the reaction  $ep \rightarrow eX$  with the structure function  $F_2(x)$  for the reaction  $K^+ p \rightarrow K^0 X$ , calculated under the assumption of a dominant contribution from  $\rho$ -meson exchange according to the equation

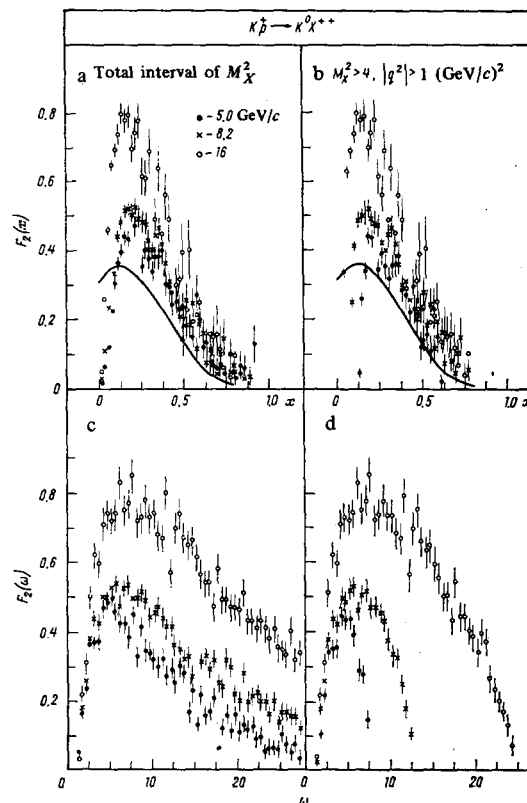


FIG. 22. The structure function  $F_2$  as a function of the variables  $x$  and  $\omega = 1/x$  for all events (a, c), and after separating the resonance region (b, d). The points show the data for the reaction  $K^+ p \rightarrow K^0 X$  at 5, 8.2, and 16 GeV/c; the solid curves show the SLAC data for the reaction  $ep \rightarrow eX$  (from Ref. 84).

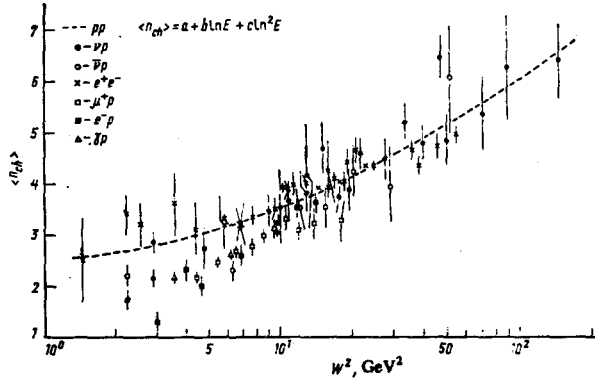


FIG. 23. The average multiplicity of secondary charged hadrons as a function of  $W^2$ . The points show a compilation of data. [12]

$$\frac{d^2\sigma}{dx dy} = \frac{v_p^2 K K}{4\pi} \frac{4m_p E_p}{q^2 - m_p^2} [1 + (1-y)^2] F_2(x, y), \quad (4.20)$$

where  $x = 1/\omega = -q^2/2m_p\nu$ ,  $y = \nu/E_0$ , and  $\nu = E - E_0$  is the energy loss. It can be seen from Fig. 22 that there is actually relatively good agreement between the structure functions for these two reactions in the region  $x \sim 1$ .

A comparison of the average multiplicities of hadrons produced in lepton-hadron, electromagnetic, and hadron-hadron interactions at identical values of the total energy  $W$  available for hadron production (Fig. 23) also suggests the existence of a deep analogy between these interactions.

Such a relation to deep inelastic scattering arises in a natural way in models in which particle production occurs through the fusion of quarks from different hadrons, in analogy with the well-known Drell-Yan mechanism of lepton pair production in hadron-hadron interactions [85] (Fig. 24). According to these quark fusion models, the inclusive cross section for the production of a meson of mass  $m_c$  has the form [86]

$$f \approx \frac{A}{m_c^2} f_q^a(x_1) f_q^b(x_2), \quad (4.21)$$

where  $f_{q(a)}^{a(b)}$  is the distribution function for quarks (antiquarks) in the hadron  $a(b)$ , and

$$x_{1,2} = \frac{1}{2} \left( \frac{1}{s} \sqrt{x_c^2 + \frac{4m_c^2}{s}} \pm x_c \right) \quad (4.22)$$

or  $x_{1,2} = m_c e^{\pm y} / \sqrt{s}$ .

In the fragmentation region of the hadron  $a$ , we have  $x_c \sim 1$ ,  $x_1 \sim x_c$ , and  $x_2 \sim m_c^2/sx$ . Therefore

$$f \xrightarrow{x_c \rightarrow 1} \frac{A}{m_c^2} f_q^a(x_c) f_q^b\left(\frac{m_c^2}{sx}\right). \quad (4.23)$$

Owing to the fact that a hadron contains a "sea" of quark-antiquark pairs ( $f_q(0) \neq 0$ ), this gives [87]

$$f \xrightarrow[x_c \rightarrow 1, s \rightarrow \infty]{} \frac{A}{m_c^2} f_q^a(x_c) \sim (1-x)^n, \quad (4.24)$$

where  $n = 3$  for the proton.

In this model, the inclusive cross section is given by

a sum of factorized terms of the type (4.21). This means that it would also be of interest to take into account higher-order terms in the expansion in powers of  $\gamma$  in the representation (4.17) proposed by Logunov *et al.* In this sense, Eq. (4.17) can evidently be regarded as a first approximation, which is dominant in the region of large  $\gamma$ .

The "fusion" mechanism predicts different rates of approach to the scaling limit in the fragmentation and central regions. In fact, according to (4.23) for the fragmentation region, the term which violates the scaling limit depends on  $m_c^2/sx$ , whereas in the central region we have

$$f = \frac{A}{m_c^2} f_q\left(\frac{m_c}{\sqrt{s}}\right) f_q\left(\frac{m_c}{\sqrt{s}}\right) \quad (4.25)$$

and an energy dependence appears only through the variable  $m_c/\sqrt{s}$ . It is important to note that in both cases the scale of energies is given by the mass  $m_c$  of the produced particle (or by the transverse mass  $\langle m_{Tc} \rangle$  if allowance is made for the transverse motion of the partons) and the inclusive cross section has a certain universal dependence [88] on the variable  $m_c/\sqrt{s}$ :

$$f(p_c, s) \approx \frac{A}{m_c^2} G\left(\frac{m_c}{\sqrt{s}}, x\right). \quad (4.26)$$

For light particles, large numbers of which are produced as a result of the decays of various resonances, this scaling law may be violated because of the existence of several scales of mass. Nevertheless, as we can see from Fig. 25, the average multiplicities of different types of particles produced in  $pp$  collisions yield a single curve starting at the Serpukhov energies, after introducing a simple redefinition of the scale of energies and a change in the overall normalization [89]; this may indicate the existence of a single effective mechanism that dominates at high energies. The cross sections for the production of resonant states ( $\rho$ ,  $\varphi$ ,  $\psi$ ) in  $pp$  interactions also exhibit a universal dependence on the variable  $m_c^2/s$  which is close to that obtained from the Drell-Yan mechanism (Fig. 26).

The fact that the scale of energies in the inclusive distributions is given by the average transverse mass may lead (as pointed out at the end of Sec. 4b) to an earlier deviation of the inclusive cross sections for light particles in the central region from the predictions of the Regge pole model, owing to the same mechanism that is responsible for the growth of the total cross sections.

## 5. INCLUSIVE RESONANCE PRODUCTION

The preceding sections were concerned mainly with the description of the stable-particle spectra and had little to say about the production of resonant states.

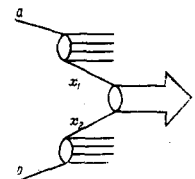


FIG. 24. Mechanism of particle production by the fusion of quarks from the interacting hadrons.



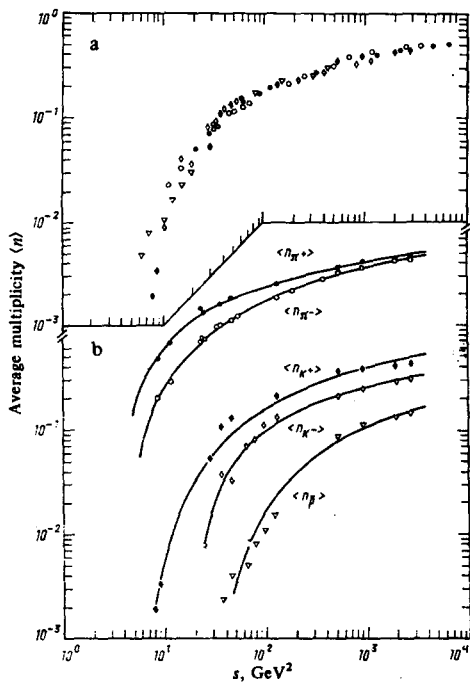


FIG. 25. The average multiplicities of  $\pi^+$ ,  $K^+$ , and  $\bar{p}$  as a function of  $s$  (b), and the same data as in (b) but displaced to the average multiplicity of  $K^+$  mesons (a). The displacements along the  $\langle n \rangle$ -axis are proportional to the ratios of the corresponding masses squared (from Ref. 89).

However, we note that it is necessary to consider the latter in order to be able to understand the degree of violation of  $SU(3)$  or  $SU(6)$  symmetry in multi-particle production processes. In fact, as we showed in the preceding sections, the cross section for kaon production in the studied range of energies is an order of magnitude smaller than the cross section for pion production, and there is no evidence that these cross sections become equal asymptotically. On the contrary, many approximations show that this relationship is preserved at higher energies. Thus it might be said that there is a strong violation of  $SU(3)$  symmetry in multi-particle production processes.

However, as shown by Anisovich and Shekhter<sup>[91]</sup> and subsequently by Bjorken and Farrar,<sup>[92]</sup> such a strong symmetry breaking is only apparent and is due to the fact that experiments are performed to detect only stable particles, some of which are actually produced as a result of the decays of resonant states. Allowance for the decays of resonances restores the symmetry. For example, by allowing for the contributions from the lowest  $SU(6)$  multiplets (the 36-plet of mesons and the 56-plet of baryons), it is possible to give a qualitative explanation of the existing relations between the yields of stable particles at finite energies, even though these predictions are asymptotic and do not take into account the suppression in the production of heavy particles. Such a suppression should be expected from simple multiperipheral kinematics, according to which the cross sections for particle production depend on the transverse masses of the particles. As we showed in the preceding section, the cross sections for producing heavy particles according to the quark fusion mechanism

are also suppressed like  $1/m_c^2$  (see Eq. (4.26)). The same suppression factor appears in the parton model as a result of the short range of the quarks in rapidity space.<sup>[87]</sup> In fact, the probability of finding a  $q\bar{q}$  pair with a (quark-antiquark) rapidity difference  $\Delta y \approx \ln(m_c^2/m_q^2)$  is proportional to  $e^{-\alpha\Delta y}$ , which leads to a suppression factor  $1/m_c^{2\alpha}$  in the cross section for the production of a particle of mass  $m_c$ .

We point out another circumstance which is not taken into account in the asymptotic quark model. According to the fusion mechanism, the probability of producing a meson is proportional to the probability of finding a quark in one hadron and an antiquark in the other. Experiments on deep inelastic scattering indicate that there are few antiquarks in the nucleon. There is no such suppression in a meson, which already contains a valence antiquark. This fact explains the abundance of mesons in  $\pi p$  collisions in comparison with the number of mesons in  $pp$  collisions at moderate energies. This additional contribution in the fusion model falls off like  $m_c/\sqrt{s}$  with increasing energy, and the cross sections for meson production in  $\pi p$  and  $pp$  collisions should become similar at asymptotic energies. In this connection, great care must be taken in comparing the quark model<sup>[91]</sup> with experiment at moderate energies.

Thus studies of the inclusive production of resonances (which, being, as it were, the parent particles, more accurately reflect the characteristic primary features of the interaction than the daughter particles into which they decay) are of great importance as tests of the various models describing the symmetry of quark models. Analyses of the spin density matrices characterizing the decays of resonances offer unique prospects of studying the dynamics of particle production processes. The copious production of resonances, whose decay products account for an appreciable fraction of the particles observed in the final state, seems to be intimately related to the correlation effects observed in multi-particle production processes, which suggest that many pions originate from the decay of clusters with large mass. It is becoming more and more obvious that the observed short-range correlations may actually be due to resonance production. Finally, the surprisingly large yield of direct leptons in hadron-hadron interactions has also stimulated interest in studies of meson resonances, which may be at least partially responsible for the observed effect.

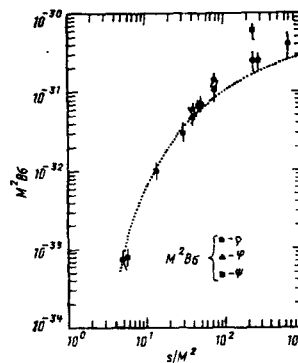


FIG. 26. Dependence of  $M^2 B \sigma$  on  $s/M^2$  (where  $M$  is the mass of the resonance and  $B$  is a normalization coefficient) for  $\rho$ ,  $\varphi$ , and  $\psi$  production in  $pp$  interactions. The dotted curve is the prediction of a model<sup>[90]</sup> of the Drell-Yan type.

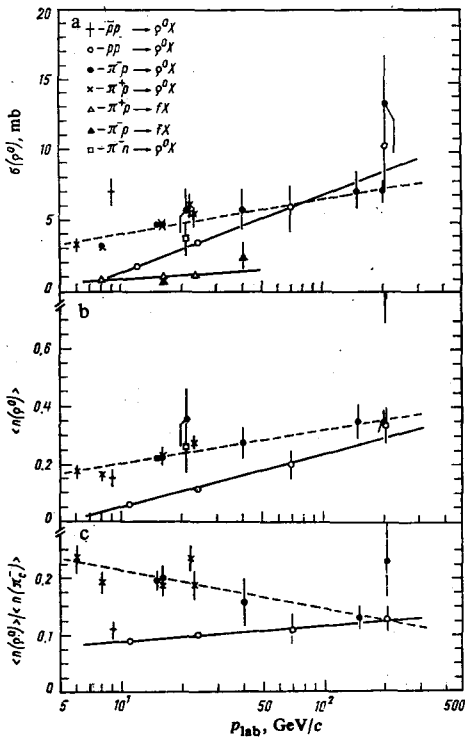


FIG. 27. Energy dependences of the inclusive cross sections for  $\rho^0$  and  $f$  mesons. a) The  $\rho^0$  and  $f$  inclusive cross sections as a function of  $p_{lab}$ ; b) the average  $\rho^0$  multiplicity as a function of  $p_{lab}$ ; c) the ratio  $\langle n(\rho^0) \rangle / \langle n(\pi^0) \rangle$  as a function of  $p_{lab}$ ; the curves are drawn through the experimental points (from a compilation<sup>[12]</sup> of published data).

#### a) Inclusive production of meson resonances

The energy dependences of the inclusive cross sections for  $\rho^0$  and  $f$  production in hadron-hadron interactions are illustrated in Fig. 27. This figure also shows the average  $\rho^0$  multiplicity in an inelastic collision and the ratio  $R = \langle n(\rho^0) \rangle / \langle n(\pi^0) \rangle$ . As in Ref. 93, we have defined  $\langle n(\pi^0) \rangle$  as the average multiplicity of produced pions, in order to allow for the strong leading-particle effect and the effects of the conservation of charge:  $\langle n(\pi^0) \rangle = \langle n(\pi^-) \rangle - 1$  for  $\pi^+p$  interactions and  $\langle n(\pi^0) \rangle = \langle n(\pi^-) \rangle$  for all other interactions. The data indicate an obvious growth of  $\sigma(\rho^0)$ ,  $\sigma(f)$ , and  $\langle n(\rho^0) \rangle$  with increasing energy, in agreement with a logarithmic dependence. The lines in the graphs a and b of Fig. 27, drawn by eye through the experimental points, correspond to

$$\sigma(\rho^0)_{pp} \sim 2.4 \ln s, \quad \langle n(\rho^0) \rangle_{pp} \sim 0.08 \ln s, \quad (5.1)$$

$$\sigma(\rho^0)_{\pi p} \sim 1.1 \ln s, \quad \langle n(\rho^0) \rangle_{\pi p} \sim 0.04 \ln s. \quad (5.2)$$

Thus there is good evidence that the energy dependence of the cross section for  $\rho^0$ -meson production is about twice as strong in  $pp$  as in  $\pi p$  interactions in the studied energy range. The ratio  $R = \langle n(\rho^0) \rangle / \langle n(\pi^0) \rangle$  rises slowly with increasing energy for  $pp$  interactions, but falls off for  $\pi p$  interactions:  $R_{\pi p} \approx 2R_{pp}$  at the minimum energies and  $R_{\pi p} \approx R_{pp}$  at the maximum energies (Fig. 27c). However, it follows from our previous discussion (see Sec. 4b) that in the asymptotic region the coefficients of  $\ln s$  in (5.1) should be independent of the

type of colliding particles and that  $R_{\pi p} = R_{pp}$ . The observed behavior must be attributed to a strong leading-particle effect in the reactions  $\pi^+p \rightarrow \rho^0 X$  (Fig. 28). In view of the empirical fact that the  $x$ -distributions for the reactions  $\pi^+p \rightarrow \rho^0 X$  and  $K^+p \rightarrow K^{*0}(890) X$  at 16 GeV/c are practically identical in the region  $x > 0.4$ ,<sup>[93]</sup> it is reasonable to assume that the fragmentation component of the  $\rho^0$ -meson cross section is equal to the total cross section for the production of the  $K^{*0}(890)$  meson, since the latter is almost entirely due to the fragmentation process. Thus the cross section for central production of the  $\rho^0$  meson can be estimated by subtracting the cross section for  $K^{*0}(890)$  production from the total inclusive cross section for the  $\rho^0$  meson. In fact, the resulting distribution (see Fig. 28) has all the features that might be expected from the central component. Thus, using this procedure, we can infer that the fragmentation production of the  $\rho^0$  meson is dominant in  $\pi^+p$  interactions at 16 GeV/c:

$$\sigma_{\text{fragm}}(\rho^0) = 3.1 \pm 0.3 \text{ mb}, \quad \sigma_{\text{central}}(\rho^0) = 1.6 \pm 0.5 \text{ mb}.$$

We have seen earlier that in the case of the reactions  $\pi^+p \rightarrow \pi^+ X$  and  $K^+p \rightarrow K^+ X$ , in which the fragmentation processes are dominant, the energy dependences of the cross sections in the central region are at first very different from those of other reactions (see Figs. 18 and 19) but become universal at higher energies. There is every reason to suppose that the same mechanism is responsible for the energy dependence of the cross sections for  $\rho^0$  production in  $\pi^+p$  interactions. We can therefore assume that asymptotically, when  $\sigma_{\text{central}}(\rho^0) > \sigma_{\text{fragm}}(\rho^0)$ , the energy dependences of  $\sigma(\rho^0)$  and  $\langle n(\rho^0) \rangle$  will be the same in  $\pi^+p$  interactions as in  $pp$  interactions. In the language of the quark fusion model, the relation  $R_{\pi p} > R_{pp}$  at low energies is a consequence of the large contribution from the valence antiquark in the pion, which falls off with increasing energy. If we assume that the value of the ratio  $R \approx 0.12$  at the highest energies is close to its asymptotic limit, as indicated by the approximate equality  $R_{\pi p} \approx R_{pp}$ , the result is inconsistent with the predictions of the quark model,<sup>[91]</sup> according to which  $R = 0.18$ . By introducing a suppression factor

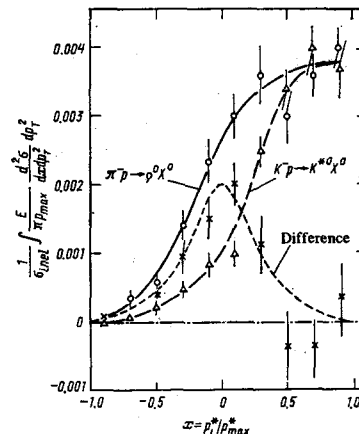


FIG. 28. Invariant  $x$ -distributions of  $\rho^0$  mesons in  $\pi^+p$  interactions and  $K^{*0}(890)$  mesons in  $K^+p$  interactions at 16 GeV/c and their difference (from Ref. 93).

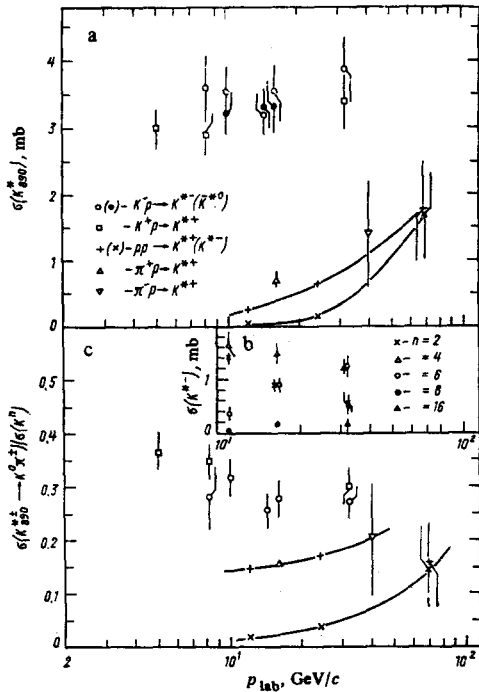


FIG. 29. Energy dependences of the cross sections for the  $K^*(890)$  resonance. a) Inclusive  $K^*(890)$  cross section as a function of  $p_{lab}$ ; b)  $\sigma(K^*(890))$  in  $K^-p$  interactions as a function of  $p_{lab}$  for various multiplicities<sup>[95]</sup>; c) the fraction of  $K^n$  mesons ( $K^0 + \bar{K}^0$ ) from the decays of  $K^*(890)$  or  $\bar{K}^*(890)$  in  $K^*p$  interactions as a function of  $p_{lab}$  (from a compilation<sup>[12]</sup> of published data).

$1/m_c^2$  for the production of a particle of mass  $m_c$ , one finds<sup>[94]</sup> the ratio  $R \approx 0.07$ , while allowance for the transverse motion leads to the bounds

$$0.07 < R < 0.18.$$

Figure 29 shows the data on the energy dependence of the cross sections for the  $K^*(890)$  resonance. In  $\pi p$  and  $pp$  interactions, the cross sections for  $K^*(890)$  production are appreciably smaller than the  $\rho^0$ -meson cross sections, but are rising rapidly with increasing energy. In  $K^*p$  interactions, we find copious production of the  $K^*(890)$  resonance, which is characterized by a weaker energy dependence than in  $pp$  interactions. The cross section for  $K^*(1420)$  production is small and is estimated to be at most 10% of the  $K^*(890)$  cross section. Most of the  $K^*(890)$  mesons in  $K^*p$  interactions are produced in events with small multiplicity (Fig. 29b), but the contribution from large topologies rises with increasing energy. Figure 29c shows the energy dependence of the ratios of the yields of neutral kaons produced as decay products of  $K^*(890)$  resonances to the total yield of neutral kaons. At Serpukhov energies, appreciable numbers of kaons are produced in  $\pi p$  and  $pp$  interactions as decay products of the  $K^*(890)$ , and the production of such kaons rises with increasing energy. In  $K^*p$  interactions, approximately 50% of all the neutral kaons are decay products of the  $K^*(890)$  (if allowance is made for the cross section for the production process  $K^*(890) \rightarrow K^0 \pi^0$ ; it can be seen from Fig. 29a that  $\sigma(\bar{K}^{*0}(890)) \approx \sigma(K^{*0}(890))$  for  $K^*p$  interactions). Within

the rather large experimental errors, the ratio  $\sigma(K^*(890) \rightarrow K^n \pi) / \sigma(K^n)$  in  $K^*p$  interactions is independent of energy. It would be of definite interest to measure this dependence more accurately over the range of energies from 10 to 100 GeV, in view of the strong growth of the cross sections for  $K^n$ -meson production at Serpukhov energies (see Sec. 3) and the marked growth of the  $K^*(890)$  cross sections. In particular, in the case of pair production of strange particles, one of them (or both, at higher energies) may be decay products of a heavier resonance. Such an effect is already observed at relatively low energies. For example, the Scandinavian Collaboration<sup>[96]</sup> found appreciable production of the  $\Sigma^*(1385)$  and  $K^*(890)$  resonances in a study of the reactions  $pp \rightarrow (AK^0) + X$  and  $pp \rightarrow (K^0 \bar{K}^0) + X$  at 19 GeV/c. It is possible that the strong growth of the cross sections for  $K^n \bar{K}^n$  pair production in  $K^*p$  interactions over the range from 16 to 32 GeV/c can be attributed, at least in part, to the onset of pair production of  $K^*(890)$  resonances, although this effect still seems to be small at Serpukhov energies. The energy dependences of the average multiplicities of  $K^n$  and  $K^*(890)$  mesons in  $K^*p$  interactions are shown in Fig. 30. The  $K^n$  and  $K^*(890)$  cross sections are larger in  $K^-p$  than in  $K^*p$  interactions, but the average numbers of both  $K^n$  and  $K^*(890)$  mesons produced in a single inelastic  $K^*p$  or  $K^-p$  interaction are approximately the same.

The energy dependences of the production cross sections and of the average multiplicities of  $K^*(890)$  mesons in  $K^*p$  interactions (Figs. 29 and 30) are similar in character to those observed for  $\rho^0$  mesons in  $\pi p$  interactions. This can be explained by the fact that the  $K^*(890)$  and  $\rho^0$  mesons have similar masses, and large numbers of these mesons are produced in fragmentation processes. In fact, most of the  $K^*(890)$  mesons are produced in the forward hemisphere (Fig. 31). There is no evidence for appreciable  $K^*(890)$  production by fragmentation of the proton, and it appears that only small numbers of  $K^*(890)$  mesons are produced in central collisions. However, on the basis of data obtained by the France-USSR and CERN-USSR Collaborations at 32 GeV/c, we can assume that the central production of

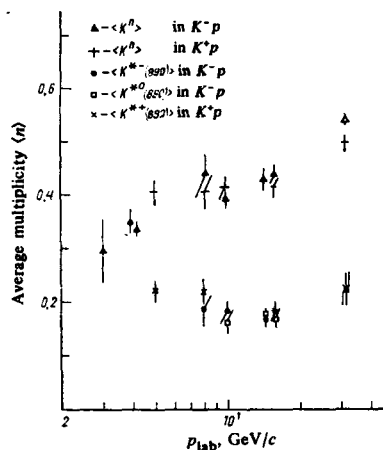


FIG. 30. Average  $K^n$  and  $K^*(890)$  multiplicities in inelastic  $K^*p$  and  $K^-p$  interactions. The points are from a compilation<sup>[12]</sup> of published data.

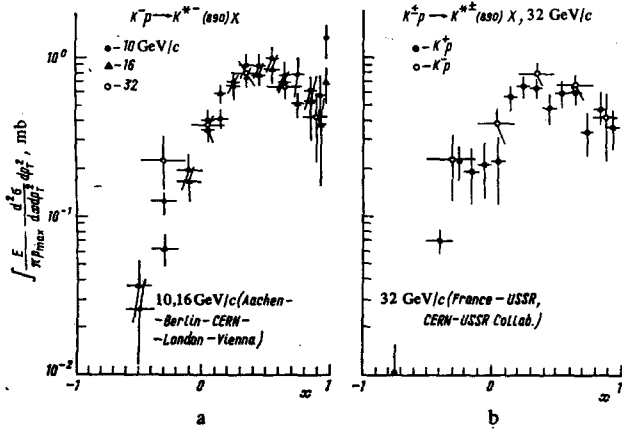


FIG. 31. Invariant  $x$ -distributions of  $K^*(890)$  resonances produced in  $K^+p$  and  $K^-p$  interactions in the reaction  $K^-p \rightarrow \bar{K}^{*0}(890)X$  at 10, 16, [97] and 32 GeV/c (a) and in the reactions  $K^+p \rightarrow K^{*+}(890)X$  and  $K^-p \rightarrow \bar{K}^{*0}(890)X$  at 32 GeV/c (b). [95,98]

$K^*(890)$  mesons has begun to rise and will be appreciably stronger at the energies of future experiments using the BEBC chamber. In the fragmentation region of the kaon, the reactions  $K^+p \rightarrow K^{*+}(890)X$  and  $K^-p \rightarrow \bar{K}^{*0}(890)X$  can take place via the exchanges  $\pi$ -B,  $\rho$ - $A_2$ , and  $\omega$ - $f$  with isospin  $I=0$  and  $I=1$  and opposite parities.

The elements of the spin density matrix (Table VI) suggest that these reactions have an appreciable contribution from pion exchange, which, as is well known, is dominant in these reactions at lower energies. [99,100] The ratios of the unnatural-parity exchanges  $\sigma^- = \rho_{00} + \rho_{11} - \rho_{1-1}$  to the natural-parity exchanges  $\sigma^+ = \rho_{11} + \rho_{1-1}$  for both values of the helicity of the  $K^*$  meson ( $\lambda=0$  and  $\lambda=1$ ) suggest a large contribution from unnatural-parity exchanges for  $|t_{KK^*}| < 1$  (GeV/c)<sup>2</sup> and  $(M^2/s) < 0.5$ , although appreciable numbers of  $K^*$  mesons in both reactions come from natural-parity exchanges. Within the accuracy of the experimental data, the inclusive  $x$ -distributions of  $K^*$  mesons in  $K^*$  interactions have approximately the same shape (see Fig. 31b) and, crudely speaking, are in the same ratio as the total inelastic cross sections for  $K^+p$  and  $K^-p$  interactions.

In Fig. 32 we compare the distributions of neutral kaons with respect to  $p_T^2$  in the reaction  $K^-p \rightarrow K^0X$  at three energies with the corresponding  $K^{*0}(890)$  distributions in the reaction  $K^-p \rightarrow \bar{K}^{*0}(890)X$ . The distributions in  $p_T^2$  for both  $K^0$  and  $\bar{K}^{*0}(890)$  mesons have little energy dependence in the interval from 10 to 32 GeV/c. They

TABLE VI. Elements of the spin density matrix of the  $K^{*0}(890)$  resonance in  $K^+p$  reactions at 32 GeV/c for  $|t_{KK^*}| < 1$  (GeV/c)<sup>2</sup> and  $M^2_X/s < 0.5$ . [95,98]

Reaction	$\rho_{00}$	$\rho_{1-1}$	Re $\rho_{10}$	$\frac{\rho_{00} + \rho_{11} - \rho_{1-1}}{\rho_{11} + \rho_{1-1}}$
$K^+p \rightarrow K_{890}^{*+}X$	$0.45 \pm 0.08$	$-0.02 \pm 0.08$	$-0.03 \pm 0.07$	$2.9 \pm 1.1$
$K^-p \rightarrow \bar{K}^{*0}(890)X$	$0.42 \pm 0.10$	$0.07 \pm 0.08$	$-0.07 \pm 0.06$	$1.8 \pm 0.6$

are not exponential, and the change in their slopes in the region  $p_T^2 \approx 0.4$  (GeV/c)<sup>2</sup> is particularly noticeable for  $K^0$  mesons. A characteristic feature of these spectra is that the ratio  $K^*/K^0$  is close to unity for  $p_T^2 \geq 1$  (GeV/c)<sup>2</sup>, while this ratio is only about 0.2 at the minimum values of  $p_T^2$ . The slope of the  $p_T^2$  spectrum is appreciably higher for  $K^0$  mesons from  $K^{*0}(890)$  decay than for all  $K^0$  mesons. [97] This indicates that mainly "direct"  $K^0$  mesons not associated with the production of  $K^*$  resonances are produced at large  $p_T^2$ , while "indirect"  $K^0$  mesons contribute mainly at small  $p_T^2$ , leading to large slopes of the  $p_T^2$  spectra at small  $p_T^2$ .

The regularities in the spectra of  $K^0$  and  $K^*(890)$  mesons in  $K^+p$  interactions that were rated above show up even more distinctly in a comparative analysis of the spectra of  $\pi$  and  $\rho^0$  mesons in  $\pi p$  collisions, for which the accessible range of energies is much higher. The distributions in  $p_T^2$  for  $\pi$ ,  $\rho^0$ , and  $f$  mesons in  $\pi p$  interactions at 16 GeV/c and for  $\pi^+$  and  $\rho^0$  mesons in  $\pi^+p$  interactions at 200 GeV/c are shown in Fig. 33. The peak at small  $p_T^2$  in the distributions for the  $\rho^0$  meson in  $\pi^+p$  [93,101] and  $\pi^+p$  [103] interactions at 16 GeV/c is due to an appreciable contribution from quasi-two-body reactions (it is not observed for  $\rho^0$  mesons in the central region (Fig. 33a), and it dies away rapidly with increasing energy (Fig. 33b)). The ratios  $\rho^0/\pi$  and  $K^*(890)/K^0$  are small in the region of low  $p_T^2$ , but rise to  $\approx 1$  with increasing  $p_T^2$ . This trend is very clearly pronounced in the data at 200 GeV/c, where the ratio  $\rho^0/\pi^+$  has a value  $\approx 0.02$  at the lowest values of  $p_T^2$ .

Since an appreciable fraction of pions is produced from the decay of resonances, this difference between the transverse momentum spectra of meson resonances and pions can be regarded as a consequence of the kinematics of resonance decays. This has been beautifully demonstrated by the ABCCCH Collaboration. [104] The daughter pions from the decays of the  $\omega$  and  $\eta$  reso-

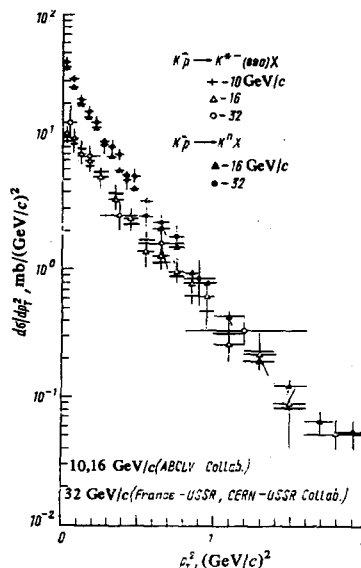


FIG. 32. The  $p_T^2$  distributions of neutral kaons in the reaction  $K^-p \rightarrow K^0X$  and of  $K^{*0}(890)$  mesons in the reaction  $K^-p \rightarrow \bar{K}^{*0}(890)X$  (the data are from Refs. 95 and 97).

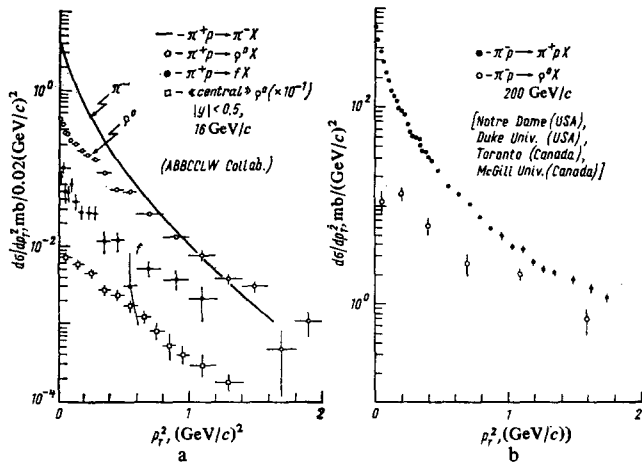


FIG. 33. The  $p_T^2$  distributions for  $\pi^-$ ,  $\rho^0$ , and  $f$  mesons in  $\pi^+p$  interactions at 16 GeV/c<sup>[101]</sup> (a) and for  $\pi^+$  and  $\rho^0$  mesons in  $\pi^-p$  interactions at 200 GeV/c (b).<sup>[102]</sup>

nances produced in the quasi-inclusive reactions

$$\pi^+p \rightarrow \omega + \text{charged particles}, \quad (5.3)$$

$$\pi^+p \rightarrow \eta + \text{charged particles}, \quad (5.4)$$

have much steeper  $p_T^2$ -distributions than the  $\omega$  and  $\eta$  resonances, whereas the  $p_T^2$  distribution of  $\pi^-$  mesons from the decay of the  $f$  resonance is very similar to the corresponding  $p_T^2$ -distribution of  $f$  mesons (Fig. 34). The values of the exponential channels for the  $p_T^2$ -distributions of  $\omega$ ,  $\eta$ , and  $\rho^0$  mesons in the quasi-inclusive reactions are approximately the same, and the  $x$ -distributions of  $\omega$  and  $\eta$  resonances in the reactions (5.3) and (5.4) are similar to the  $x$ -distribution of the inclusive  $\rho^0$  meson (Fig. 34e).

In Fig. 35 the distributions with respect to the rapidities in the c. m. s. and the  $p_T^2$ -distributions of daughter pions from the decays of  $\eta$ ,  $\omega$ ,  $\rho$ , and  $f$  resonances are compared with one another and with the spectra of inclusive  $\pi^-$  mesons. The rapidity distributions show clearly

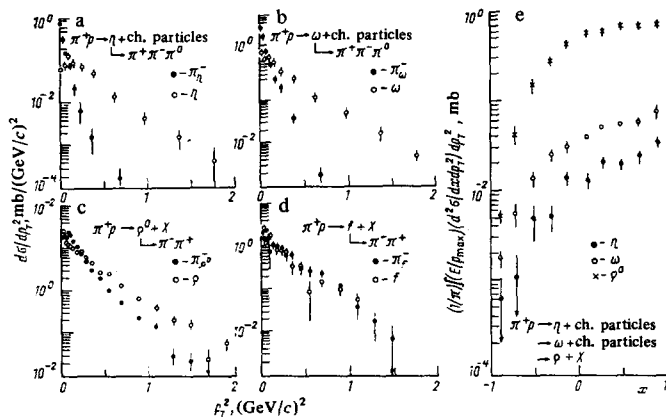


FIG. 34. The  $p_T^2$  distributions for resonances and pions from the decays of these resonances in the quasi-inclusive reactions (5.3) and (5.4) and in the inclusive reactions  $\pi^+p \rightarrow \rho^0 X$  and  $\pi^+p \rightarrow fX$  (a-d), and (e) the invariant  $x$ -distributions of  $\eta$  and  $\omega$  mesons in the reactions (5.3) and (5.4) and of  $\rho^0$  mesons in the reaction  $\pi^+p \rightarrow \rho^0 X$  (from Refs. 104 and 105).

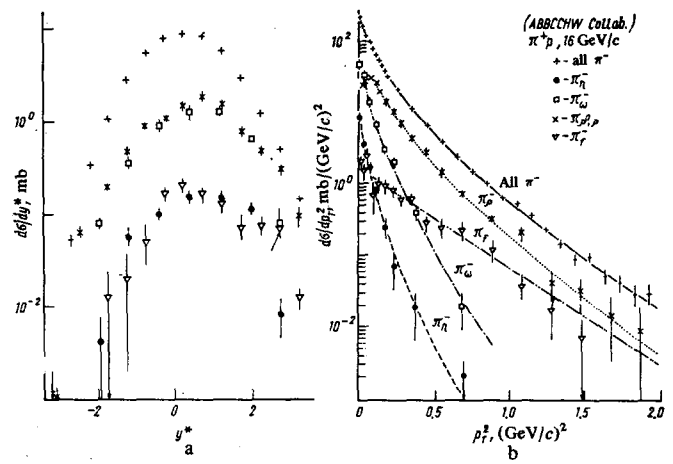


FIG. 35. Comparison of (a) the rapidity distributions of  $\pi^-$  mesons from  $\eta$ ,  $\omega$ ,  $\rho^0$ , and  $f$  decays and (b) the  $p_T^2$  distributions of  $\pi^-$  mesons from  $\eta$ ,  $\omega$ ,  $\rho^0 + \rho^-$ , and  $f$  decays with the corresponding inclusive distributions of  $\pi^-$  mesons in  $\pi^+p$  interactions at 16 GeV/c. The data are normalized to the cross sections  $\sigma(\eta) = 1.5$  mb,  $\sigma(\omega) = 4.0$  mb,  $\sigma(\rho^0) = 4.8$  mb,  $\sigma(\rho^-) = 1.6$  mb, and  $\sigma(f) = 0.63$  mb (from Ref. 104).

that the indirect pions give a large relative contribution in the fragmentation region of the beam. The contribution from  $\omega$  decay is dominant at the lowest values of  $p_T^2$ , whereas at high  $p_T^2$  the largest contribution to the indirect pions comes from  $\rho$  and  $f$  mesons.

On the basis of these experimental observations and an analysis of the exclusive channels of  $\eta$ ,  $\omega$ , and  $\rho^0$  production, it has been estimated<sup>[105]</sup> that the inclusive yields of  $\eta$ ,  $\omega$ , and  $\rho^0$  mesons in  $\pi^+p$  interactions at 16 GeV/c are given by

$$\eta:\omega:\rho^0 = 0.34:0.9:1$$

with  $\sigma(\rho^0) = 4.8 \pm 0.4$  mb,  $\sigma(\omega) = 0.4 \pm 0.6$  mb, and  $\sigma(\eta) = 1.5 \pm 0.3$  mb. These estimates are in reasonable agreement with the ratios  $\omega/\rho^0 = 1.0 \pm 0.2$  and  $1.1 \pm 0.2$  obtained in  $pp$  interactions at 12 and 24 GeV/c<sup>[106]</sup> and with new results from the CERN ISR<sup>[107]</sup> for the reaction  $pp \rightarrow ppX$  ( $X = \rho^0, \omega, f, A_2$ ) over a limited range of momentum transfers  $t_{pp1}$  and  $t_{pp2}$  and of the rapidity of the central cluster ( $y < 0.8$ ) (see, e.g., Ref. 13). In the case of  $\pi p$  interactions at 16 GeV/c, the pions from the decays of only the four resonances  $\rho, \omega, \eta$ , and  $f$  account for 46% of the total pion yield, but since the ratio  $R = \langle n(\rho^0) \rangle / \langle n(\pi) \rangle$  is decreasing with increasing energy, we might expect that this number will change at higher energies.

The production of  $\eta'$  and  $\phi$  mesons is suppressed, at least at relatively low energies. In  $\pi^+p$  collisions at 16 GeV/c, we have  $\sigma(\phi)/\sigma(\rho^0) \leq 0.025$  and  $\sigma(\eta')/\sigma(\eta) \approx 0.05-0.10$ .<sup>[108]</sup> In  $pp$  collisions at 24 GeV/c,<sup>[109]</sup> the inclusive cross section for the  $\phi$  meson has the value  $\sigma(\phi) = 0.15 \pm 0.035$  mb, with a ratio  $\sigma(\phi)/\sigma(\rho^0) = 0.045 \pm 0.012$ . However, this ratio is nearly an order of magnitude greater than the value of the ratio  $\sigma(\phi)/\sigma(\rho^0)$  which is known from the data on exclusive reactions.<sup>[109]</sup> The large cross section for  $\phi$  production in the reaction

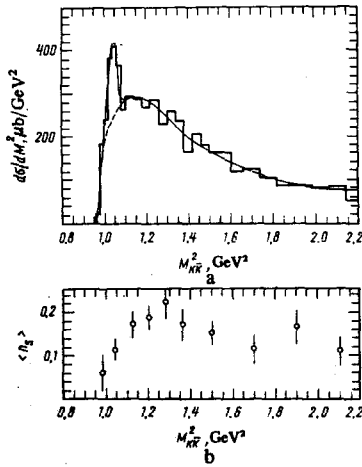


FIG. 36. Distribution with respect to the square of the  $K^*h^*$  effective mass in the  $pp$  experiment at 24 GeV/c<sup>[108]</sup> (a) (the  $K^*$  meson is identified by its decay mode, and  $h^*$  is any other unidentified hadron, which is assigned the mass of the kaon), and the average multiplicity of strange particles in an inelastic interaction with a  $K^*h^*$  pair as a function of  $M_{K^*h^*}^2 = M^2(K^*h^*)$  (b).

$pp \rightarrow \varphi + X$  at 24 GeV/c might be due to a large contribution from processes of the type  $pp \rightarrow \varphi + KK + X$ , which are allowed by Zweig's rule.<sup>6)</sup> Production of the  $\varphi$  meson is clearly seen in this last experiment in the  $K^*h^*$  effective-mass spectrum (Fig. 36a). According to Zweig's rule, we should expect  $\varphi$  production to be accompanied by an additional pair of strange particles; direct  $\varphi$  production, which is forbidden by Zweig's rule, should account for only 1% of the  $\rho^0$  cross section. However, the corresponding distribution of associated multiplicities of strange particles (with a  $K^*h^*$  pair) does not exhibit the appropriate peak in the region of the  $\varphi$ -meson mass (Fig. 36b), so that we are forced to conclude that Zweig's rule is violated in inclusive reactions.

The applicability of Zweig's rule in exclusive reactions has been established in studies of  $\varphi$  production in the reactions  $\bar{p}p \rightarrow K^*K^*K^*K^*$  and  $\bar{p}p \rightarrow K^*K^*\pi^+\pi^-$  at 3.6 GeV/c.<sup>[110]</sup> The absence of events with small  $p\omega$  masses in the reaction  $K^*p \rightarrow K^*\varphi p$ , in contrast with the conspicuous peak at small  $p\omega$  masses in the reaction  $K^*p \rightarrow K^*\omega p$ , as seen in a  $K^*p$  experiment at 14.3 GeV/c<sup>[111]</sup> and beautifully illustrated by the Dalitz plots (Fig. 37), is also a direct consequence of Zweig's rule. In fact, while Zweig's rule allows the two diagrams shown in Fig. 38a, which are responsible for the production of  $p\omega$  systems with small masses in the reaction  $K^*p \rightarrow K^*\omega p$ , the corresponding diagrams involving  $\varphi$  production in the reaction  $K^*p \rightarrow K^*\varphi p$  are forbidden by this rule, according to which the  $pp\varphi$  vertex cannot occur. However, the production of  $K^*\varphi$  systems with small masses is allowed by the two lowest-order diagrams shown in Fig. 38b, and these systems are actu-

<sup>6)</sup> Zweig's rule forbids processes in which quarks of one type annihilate into quarks of another type ( $s\bar{s} \rightarrow u\bar{u}, d\bar{d}; c\bar{c} \rightarrow u\bar{u}, d\bar{d}, s\bar{s}$ ) and accounts for the small widths of the decays of  $\varphi$  and  $\psi$  mesons into ordinary hadrons. In the case of processes involving  $\varphi$  production, this rule allows transitions in which the  $\varphi$  meson is accompanied by strange particles.

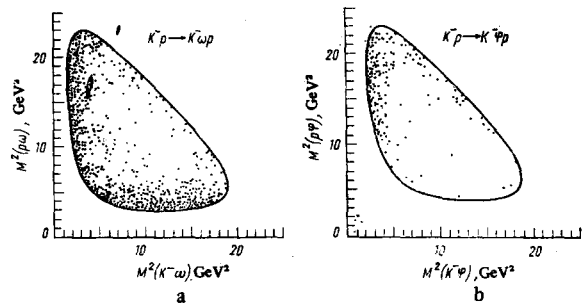


FIG. 37. Dalitz plots for the reactions  $K^*p \rightarrow K^*\omega p$  (a) and  $K^*p \rightarrow K^*\varphi p$  (b) at 14.3 GeV/c.<sup>[111]</sup>

ally observed experimentally. Studies of  $\varphi$  and  $\omega$  production in the exclusive channels in  $\pi p$ ,  $Kp$ , and  $pp$  interactions at 10 GeV/c<sup>[112]</sup> also indicate the validity of Zweig's rule.

Thus  $\varphi$  mesons are produced in  $pp$  interactions at 24 GeV/c mainly through processes that violate Zweig's rule, but for some unknown reason this violation is stronger in inclusive reactions than in exclusive reactions. The problem is aggravated by the fact that the ratio  $\sigma(\varphi)/\sigma(\rho^0 + \omega)$ , measured in a  $\pi^*p$  experiment at 43 GeV/c at Serpukhov,<sup>[113]</sup> has the value  $(4.8 \pm 2.7) \times 10^{-3}$  for  $x > 0.4$ , i. e., it is in better agreement with the exclusive data than the result of the  $pp$  experiment at 24 GeV/c. This problem obviously requires a more thorough experimental investigation.

As we should expect from naive quark arguments, the cross section for  $\varphi$ -meson production in  $K^*p$  interactions measured at Serpukhov at 43 GeV/c<sup>[113]</sup> by analyzing the spectrum of  $\mu^+\mu^-$  pairs (Fig. 39c) was found to be much larger than in  $pp$  and  $\pi p$  interactions and has the value  $0.43 \pm 0.11$  mb for  $x > 0.4$ . It can be seen from Fig. 39a that the  $x$ -distribution in the reaction  $K^*p \rightarrow \varphi X$  is well described by the dependence  $1 - x$ , which follows from the quark fusion mechanism discussed above and the quark counting rules.<sup>[114]</sup> Analogous dependences  $(1 - x)^n$  for the spectra of  $\rho^0$ ,  $\omega$ , and  $J$  mesons have been observed in  $\pi Fe$  and  $p Fe$  interactions at 200 and 240 GeV/c,<sup>[115]</sup> with  $n=3$  and  $n=1$  for  $p Fe$  and  $\pi Fe$  interactions, respectively.

The suppression of  $\varphi$  and  $\eta'$  production represents another serious problem for simple quark models,<sup>[91, 92]</sup> as can easily be seen by comparing the model predictions with the results of the  $\pi^*p$  experiment at 16 GeV/c<sup>[101]</sup> (Table VII). If we introduce a suppression coefficient  $\sim (M^2)^{-1}$  for a meson of mass  $M$ , as discussed earlier in connection with the quark fusion mechanism, the situation is improved somewhat, but only slightly.

Since the observed pions are frequently decay products of resonances, we must distinguish the pions

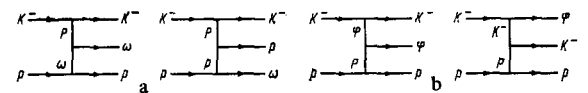


FIG. 38. Double-reggeon diagrams corresponding to the near-threshold peaks in the  $p\omega$  (a) and  $K^*\varphi$  (b) effective-mass spectra in the reactions  $K^*p \rightarrow K^*\omega p$  and  $K^*p \rightarrow K^*\varphi p$ , respectively.

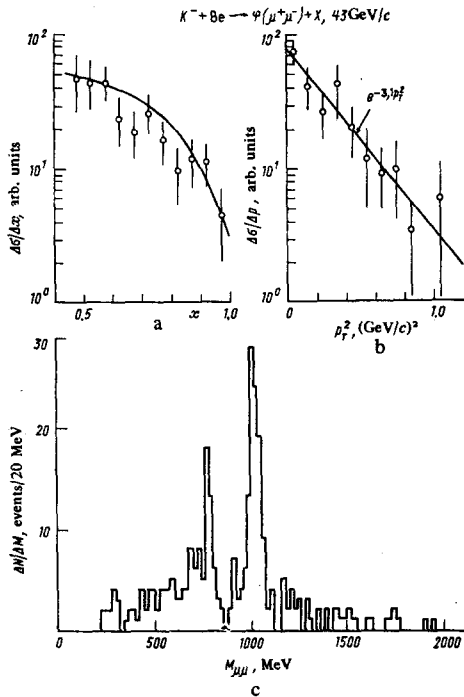


FIG. 39. The  $\mu^+\mu^-$  effective-mass spectrum in the reaction  $K^- + \text{Be} \rightarrow \varphi(\mu^+\mu^-) + X$  at  $43 \text{ GeV}/c$  <sup>[113]</sup> (c) and the distributions of  $\varphi$  mesons with respect to  $x$  and  $p_T^2$ , a) The dependence  $1 - x$ ; b) the dependence  $\exp(-3.1p_T^2)$ .

which are produced directly from those which originate from the decays of other particles. The estimate of the proportion of direct pions,  $\pi_{\text{dir}}/\pi_{\text{all}}$ , obtained from the  $\pi p$  experiment <sup>[101]</sup> by simply summing the contributions of all the known resonances to the total inclusive cross section for pions in the reaction  $\pi^+p \rightarrow \pi^- + X$  is also inconsistent with the predictions of the quark model (see Table VII), provided that the production of baryon resonances is not responsible for a larger fraction of indirect pions than that to which we are accustomed.

#### b) Inclusive production of baryon resonances

Most of the available information on the inclusive cross sections for baryon resonances comes from studies of the production of the  $\Delta^{++}(1236)$  and  $\Delta^0$  isobars in bubble-chamber experiments. Therefore the data are confined mainly to the fragmentation region of the proton, where the slow protons from the decay of the isobar can be identified by their ionization. To some extent, the determination of the cross section for the  $\Delta^{++}(1236)$  isobar is arbitrary, since the  $\Delta^{++}$  is a broad resonance and various methods are in common use in estimating the

TABLE VII. Ratios of the cross sections for producing non-strange mesons in  $\pi^+p$  interactions at  $16 \text{ GeV}/c$  <sup>[101]</sup> and the predictions of the simple quark model. <sup>[91]</sup>

Ratio	Experiment	Prediction	Ratio	Experiment	Prediction
$\omega/\rho^0$	$\approx 1$	1	$\eta'/\eta$	0.05—0.010	19/11
$\eta/\omega$	$0.39 \pm 0.03$	11/81	$\pi_{\text{dir}}/\pi_{\text{all}}$	0.15—0.5	0.07
$\varphi/\rho^0$	$\leq 0.025$	1/9			

background. Nevertheless, the characteristic features of the energy dependence of the  $\Delta^{++}(1236)$  cross section can be clearly seen in Fig. 40. For the non-exotic reactions (in the sense of the channel  $abc$ ) in  $pp$ ,  $\pi^+p$ , and  $K^+p$  interactions, the cross sections fall off at about the same rate in the low-energy region. The ratios of the cross sections for these reactions in this region at fixed  $s$  are consistent with the ratios of the total inelastic  $pp$ ,  $\pi^+p$ , and  $K^+p$  cross sections and are therefore consistent with factorization.

The  $\Delta^{++}(1236)$  cross sections in  $pp$  interactions above  $100 \text{ GeV}/c$  are practically independent of energy and equal to about  $1.5 \text{ mb}$ . A study of  $\Delta^{++}$  production at CERN ISR energies has shown <sup>[116]</sup> that the  $\Delta^{++}$  cross section in the region  $0 < p_T < 0.7 \text{ GeV}/c$  and  $x > 0.6$  is practically the same at the energies  $\sqrt{s} = 23 \text{ GeV}$  and  $\sqrt{s} = 35 \text{ GeV}$ :

$$\frac{\sigma(\sqrt{s} = 23 \text{ GeV})}{\sigma(\sqrt{s} = 35 \text{ GeV})} = 1.03 \pm 0.03.$$

Within a limited range of the variables ( $1.16 < M(p\pi^+) < 1.32 \text{ GeV}$ ,  $0.86 < x < 0.92$ , and  $0.1 < -t < 0.5 \text{ GeV}^2$ ) at  $\sqrt{s} = 30.4 \text{ GeV}$ ,  $\Delta^{++}$  production in the same experiment is in agreement with a dominant contribution from single-pion exchange and, in particular, with the Chew-Low model modified by the introduction of a Dürr-Pilkuhn form factor. Integration over the entire range of the variables gave a cross section independent of  $s$  and having the value  $\sigma(\Delta^{++}) = 4.5 \text{ mb}$  in both hemispheres. This result is consistent with bubble-chamber data at energies above  $100 \text{ GeV}$ , where the use of a cut-off in  $t$  significantly reduces the actual cross section for the  $\Delta^{++}$  isobar.

For the exotic  $\pi^-p$  and  $K^-p$  reactions we should expect no energy dependence even at low energies. With-in the limited statistics, the data are consistent with this assumption. This trend is clearly seen over a wide range of energies in the case of  $\pi^-p$  collisions, where all the experimental data have been obtained in a similar manner. A very crude comparison of the trend of the data for the non-exotic  $K^+p$  and  $\pi^+p$  reactions with the

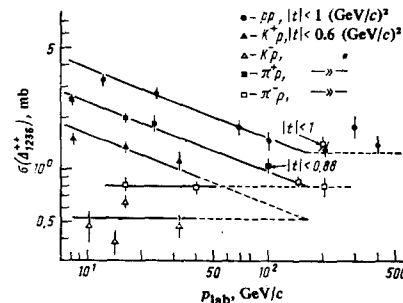


FIG. 40. The inclusive  $\Delta^{++}_{1236}$  cross section as a function of the primary momentum;  $\Delta^{++}$  is defined in the mass band  $1.12 < M(p\pi^+) < 1.32 \text{ GeV}/c^2$  (with small differences in certain experiments) with the indicated cuts in  $t$ . However, the backgrounds in different experiments were estimated by different methods. Certain experiments used the Breit-Wigner procedure to obtain the  $\Delta^{++}$  cross section (the points are from a compilation <sup>[12]</sup> of published data).

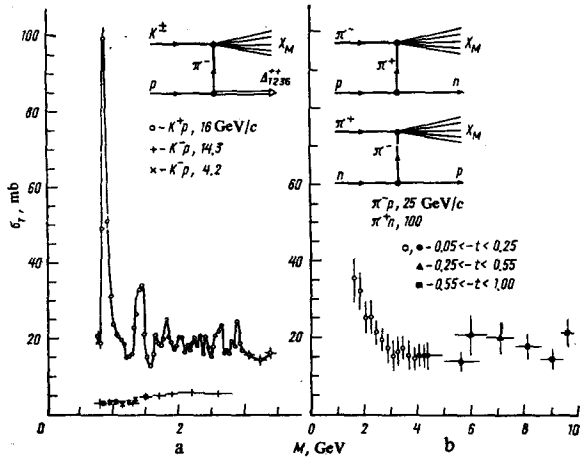


FIG. 41. Total cross sections for the  $K^+\pi^-$ ,  $K^-\pi^-$ , and  $\pi^+\pi^-$  interactions obtained from analyses of the reactions  $K^+p \rightarrow \Delta^{++}X$ ,  $n^-p \rightarrow nX$ , and  $\pi^+n \rightarrow pX$  as a function of the mass of the system  $X$  (i.e., the energy of the  $K\pi$  or  $\pi\pi$  system in its rest frame) (the data are from Refs. 117–121).

corresponding constant cross sections for the  $K^+p$  and  $\pi^+p$  reactions shows that the energy dependence of the cross sections for  $\Delta^{++}$  production in  $K^+p$  and  $\pi^+p$  interactions should develop a plateau at energies above 100 GeV, as observed in  $pp$  collisions. Of course, the actual energy dependences of the  $\Delta^{++}$  cross sections for reactions initiated by various primary particles may be somewhat different from what is expected on the basis of a simple extrapolation of the data at low energies. This energy dependence is determined by the leading exchange mechanisms.

Analyses of the angular distributions and the elements of the  $\Delta^{++}(1236)$  spin density matrix in a number of experiments have made it possible to establish that single-pion exchange plays a dominant role for small  $|t|$ , even at the CERN ISR energies. For example, an extrapolation to the pion pole by means of the Chew-Low equation in the reaction  $pp \rightarrow \Delta^{++}(1236)X$  at  $\sqrt{s} = 30.4$  GeV<sup>[116]</sup> yielded values of  $\sigma_{\text{tot}}(\pi^+p)$  in the range from  $21.1 \pm 0.5$  mb to  $21.1 \pm 1.3$  mb (using different extrapolation procedures), in good agreement with the actual value  $\sigma_{\text{tot}}(\pi^+p) = 24.3$  mb. Using either a Chew-Low extrapolation to the pion pole or a reggeized single-pion model for the reactions  $K^+p \rightarrow \Delta^{++}X$ ,<sup>[117–119]</sup>  $\pi^+p \rightarrow nX$ ,<sup>[120]</sup> and  $\pi^+n \rightarrow pX$ ,<sup>[121]</sup> it has been possible to measure the total cross sections for  $K^+\pi^-$  and  $\pi^+\pi^-$  scattering (Fig. 41).

The total cross sections for  $\pi^+\pi^-$  scattering fall off rapidly from the resonance region to an asymptotic cross section at the level of 14–16 mb, in accordance with predictions based on factorization:  $\sigma_{\text{tot}}(\pi^+\pi^-) = \sigma_{\text{tot}}(\pi^+p)\sigma_{\text{tot}}(\pi^-p)/\sigma_{\text{tot}}(pp)$ . The  $K^+\pi^-$  cross sections, measured at energies up to 3.5 GeV in the c. m. s., follow the same trend, but within the accessible range of energies they are still higher than the corresponding predictions which follow from factorization. We can assume that this is due to the existence of many resonant states in the non-exotic  $K^+\pi^-$  channel. The total cross sections for  $K^+\pi^-$  scattering in the exotic  $K^-\pi^-$  channel are appreciably smaller than the cross sections

for  $K^+\pi^-$  scattering and approach their asymptotic limit from below. If the trend of the data indicated in Fig. 41 continues at high energies, we might expect the cross sections for  $\Delta^{++}$  production in the fragmentation region of the proton to become equal in  $K^+p$  interactions and in  $\pi^+p$  and  $\pi^-p$  interactions, with

$$\sigma_{\Delta^{++}}(pp) : \sigma_{\Delta^{++}}(\pi p) : \sigma_{\Delta^{++}}(Kp) = \sigma_{\text{tot}}(\pi p) : \sigma_{\text{tot}}(\pi\pi) : \sigma_{\text{tot}}(K\pi).$$

However, the contributions from other exchanges with isospin 1, such as the  $\rho$  and  $A_2$ , which can contribute to these reactions, as well as the interference between the various exchanges, may lead to appreciably different results over the entire range of momentum transfers. Moreover, a large part of the cross section for  $\Delta^{++}$  production is due to processes involving the formation and subsequent decay of the diffraction system  $p\pi^+\pi^-$ , in which the triple-reggeon parametrization and factorization of the Pomeron pole may lead to very different predictions.

There is very little experimental information about the inclusive production of the  $\Delta^0(1236)$  isobar. We know that production of the systems  $p\pi^+$  and  $p\pi^-$  with small masses is strongly correlated because of the diffraction production of the  $p\pi^+\pi^-$  system. Since the diffraction system  $p\pi^+\pi^-$  has isospin 1/2, the cross section for the process  $\Delta^{++} \rightarrow p\pi^+$  is nine times as large as the cross section for the process  $\Delta^0 \rightarrow p\pi^-$ . This accounts for the existence of the large background under the  $\Delta^0$  peak and makes it difficult to separate the  $\Delta^0$  resonance. However, to counterbalance certain conclusions, we would like to stress that the cross section for  $\Delta^0$  production may be much larger than 1/9 of the  $\Delta^{++}$  cross section, since diffraction production of the system  $p\pi^+\pi^-$  with  $I=1/2$  is by no means the only mechanism of  $\Delta^0$  production, at any rate in the studied energy range. Thus, in the region of small  $t$ , where single-pion exchange dominates, we have the following relations:

$$\frac{\sigma(pp \rightarrow \Delta^0 X)}{\sigma(pp \rightarrow \Delta^{++} X)} = \frac{\sigma_{\text{tot}}(\pi^+p)}{3\sigma_{\text{tot}}(\pi^-p)}, \quad (5.5)$$

$$\frac{\sigma(\pi^\pm p \rightarrow \Delta^0 X)}{\sigma(\pi^\pm p \rightarrow \Delta^{++} X)} = \frac{\sigma_{\text{tot}}(\pi^\pm\pi^+)}{3\sigma_{\text{tot}}(\pi^\pm\pi^-)}, \quad (5.6)$$

$$\frac{\sigma(K^\pm p \rightarrow \Delta^0 X)}{\sigma(K^\pm p \rightarrow \Delta^{++} X)} = \frac{\sigma_{\text{tot}}(K^\pm\pi^+)}{3\sigma_{\text{tot}}(K^\pm\pi^-)}. \quad (5.7)$$

For example, an experiment at 14.3 GeV/c<sup>[122]</sup> gave the results  $\sigma(\Delta^{++}) = 700 \pm 100 \mu\text{b}$  for the reaction  $K^+p \rightarrow \Delta^{++}X$ , in contrast with  $\sigma(\Delta^0) = 985 \pm 180 \mu\text{b}$  for the reaction  $K^+p \rightarrow \Delta^0 X$ . It was shown in this same experiment that the ratio (5.7) for the  $K^+p$  reactions and the ratio  $\sigma(K^+p \rightarrow \Delta^{++}X)/\sigma(K^+p \rightarrow \Delta^0 X)$ , which should be equal to 3 in the case of any exchange with isotopic spin  $I=1$ , actually have the expected values for both the  $K^+p$ <sup>[117, 122]</sup> and  $K^+p$ <sup>[118, 123]</sup> data. Thus the production and decay of the isobars  $\Delta^{++}$  and  $\Delta^0$  are responsible for an appreciable fraction of the indirect pions produced in hadron-hadron interactions.

An interesting attempt to separate the  $\Delta^{++}$  production over the entire kinematic region was made by the ABCCHLVW Collaboration in  $\pi^+p$  and  $K^+p$  experiments at 16 GeV/c.<sup>[124]</sup> Table VIII shows that the  $\Delta^{++}(1236)$  inclusive cross sections are almost twice as large as



TABLE VIII. The cross section for  $\Delta^{**}$  production and the relative contributions of the  $\Delta^{**}$  cross sections to the total inelastic cross section for various topologies in  $\pi^+p$  and  $K^-p$  experiments at 16 GeV/c. <sup>[124]</sup>

Reaction	$\sigma_{\text{inel}}$ , mb	Fraction, %				
		inclusive	2-prong	4-prong	6-prong	8-prong
$\pi^+p$	3.39	17.2	6.1	19.6	21.9	23.4
$\pi^-p$	1.41	6.6	—	7.5	10.5	18.0
$K^-p$	1.20	4.4	—	7.7	12.0	13.3

those obtained by applying the cuts  $1.12 < M(p\pi^+) < 1.34$  GeV and  $|t| < 0.6$  (GeV/c)<sup>2</sup> (shown in Fig. 40). It is interesting to note that the relative contribution of the  $\Delta^{**}$  production cross section to the total inelastic cross section grows with increasing multiplicity of the secondary particles, and from 45 to 49% of all the  $\Delta^{**}$  resonances are produced in events with  $n > 4$ . It can be seen from Fig. 42 that most of the  $\Delta^{**}(1236)$  isobars are produced in the backward hemisphere, i. e., they are produced from the fragmentation of protons. However, a small part of the cross section is due to  $\Delta^{**}$  production in the forward hemisphere. This last process is characterized by the presence of a break in the corresponding distribution  $d\sigma/dt$  at  $|t| \approx 3$  (GeV/c)<sup>2</sup> and appears to be due to other mechanisms of  $\Delta^{**}(1236)$  production, such as the exchange of baryon quantum numbers.

Owing to practical difficulties, there is only very meager information about the inclusive production of the heavier  $N^*$  isobars, which decay mainly into three-particle channels or via a cascade process. New data have been obtained on the production of the strange baryon resonance  $\Sigma^*(1385)$  in  $K^-p$  interactions (Fig. 43). The falling-off of the cross section for  $\Sigma^*(1385)$  production with increasing energy is very reminiscent of the energy dependence of the cross section for the reaction  $K^-p \rightarrow \Lambda X$  (see Fig. 4). The cross sections decrease over the interval from 4.2 to 10 GeV/c but have little variation within the range from 10 to 32 GeV/c, where the  $\Sigma^*(1385)$  cross section is very close to the  $\Sigma^-(1385)$  cross section; the latter varies little with increasing energy. It can be seen from the invariant distributions with respect to  $x$  (Fig. 44) that the  $\Sigma^*(1385)$  resonance is produced symmetrically about  $x=0$ , i. e., mainly in collisions of the central type. At fixed energy, the  $x$ -distributions for the  $\Sigma^*(1385)$  and  $\Sigma^-(1385)$  resonances

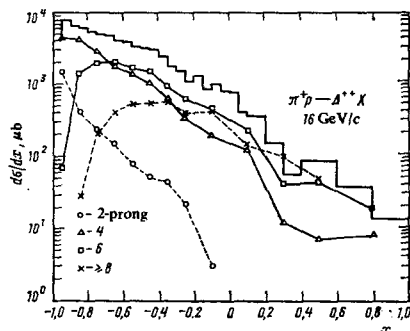


FIG. 42. Differential cross sections  $d\sigma/dx$  of the reaction  $\pi^+p \rightarrow \Delta^{**}X$  at 16 GeV/c for all events (histogram) and for various topologies (from Ref. 121).

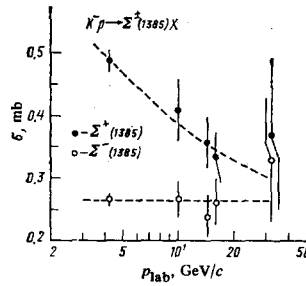


FIG. 43. Inclusive  $\Sigma^*(1385)$  cross sections in  $K^-p$  interactions as a function of the primary momentum. The data are from Refs. 95 and 125–127; the curves are drawn by eye.

are practically identical in the forward hemisphere, whereas it is found that there are significantly more  $\Sigma^*(1385)$  resonances for  $x < 0$ ; this may be attributed to quasi-two-body processes involving the exchange of hypercharge, which, as is well known, are characterized by a strong energy dependence. In fact, a triple-reggeon analysis of  $\Sigma^*(1385)$  production at 4.2 GeV/c in the fragmentation region of the proton (and hence with annihilation of strangeness at the  $K^-$  vertex) has shown<sup>[125]</sup> that the Regge trajectory responsible for the process of strangeness annihilation in the reaction  $KK^- \rightarrow$  pions is consistent with the  $f'-\varphi$  trajectory.

Information about the weak decay of the  $\Lambda$  hyperon in the two-step process  $\Sigma^*(1385) \rightarrow \pi^+ (\Lambda \rightarrow p\pi^-)$  was used by the Amsterdam-CERN-Nijmegen-Oxford Collaboration<sup>[125]</sup> to reconstruct the complete spin density matrix of the  $\Sigma^*(1385)$  resonance in the reaction  $K^-p \rightarrow \Sigma^*(1385)X$  at 4.2 GeV/c. Although the errors in the polarization are large as a result of uncertainties due to the large background, it can be deduced from the results of this experiment that the  $\Sigma^*(1385)$  polarization in the region  $|t_p, \Sigma^*| < 0.5$  (GeV/c)<sup>2</sup> is small and is consistent with zero, in agreement with the predictions<sup>[128]</sup> of the additive quark model. These results are very different from those referring to the polarization of the  $\Lambda$  hyperons in the reactions  $K^-p \rightarrow \Lambda X$ , for which it is established that the  $\Lambda$  hyperons have an appreciable polarization (see Ref. 129, where references to earlier papers can be found).

Figure 45a shows that the  $\Lambda$  hyperons for  $x < 0.5$  have significantly different polarizations in the reactions

$$K^-p \rightarrow \Lambda + \text{pions}, \quad (5.8)$$

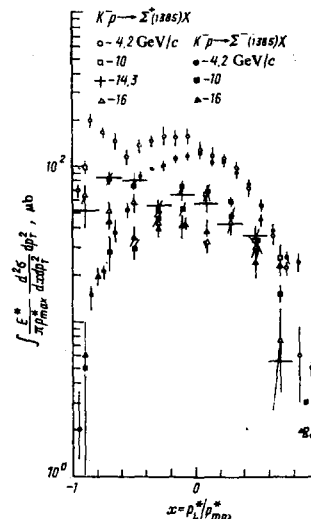


FIG. 44. Invariant  $x$ -distributions for the reactions  $K^-p \rightarrow \Sigma^*(1385)X$  (the data are from Refs. 125–127).

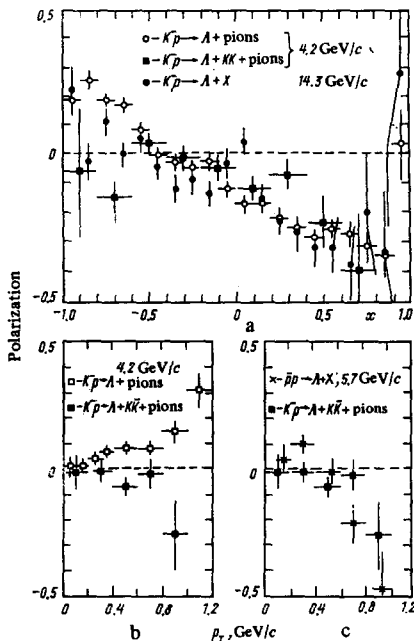


FIG. 45. The polarization of the  $\Lambda$  hyperons,  $P = (3/N) \sum_{i=1}^N q_i \cdot n_i$  (in the usual notation), as a function of the variable  $x$  in the reactions  $K^-p \rightarrow \Lambda + \text{pions}$  and  $K^-p \rightarrow \Lambda + K\bar{K} + \text{pions}$  at 4.2 GeV/c and the reaction  $K^-p \rightarrow \Lambda + X$  at 14.3 GeV/c<sup>[129]</sup> (a), and the polarization of the  $\Lambda$  hyperons with  $-1 < x < -0.2$  as a function of  $p_T$  in the reactions  $K^-p \rightarrow \Lambda + \text{pions}$  and  $K^-p \rightarrow \Lambda + K\bar{K} + \text{pions}$  at 4.2 GeV/c (b) and  $\bar{p}p \rightarrow \Lambda + X$  at 5.7 GeV/c<sup>[129]</sup> (c).



This polarization is positive for the reaction (5.8), but is slightly negative for the reaction (5.9). For events in the fragmentation region of the proton ( $-1 < x < -0.2$ ), the dependence of the polarization  $P$  on  $p_T$  (Fig. 45b) is found to be rather different for these two reactions. However, the polarization  $P$  in the reaction (5.9), which is not due to a process of strangeness annihilation, is very similar in its behavior to  $P$  in the reaction  $\bar{p}p \rightarrow \Lambda X$  (Fig. 45c). The small value of the  $\Lambda$  polarization in the fragmentation region of the proton for  $\bar{p}p$  interactions and for  $K^-p$  interactions involving the virtual process  $K\bar{K} \rightarrow K\bar{K} + \text{pions}$  may indicate that both these processes are dominated by the exchange of the Pomanchuk pole.

## 6. CONCLUSIONS

The principal results obtained from studies of inclusive and multi-particle reactions in the field of research considered in the present review can be summarized as follows.

a) The hypothesis of limiting fragmentation (due to Yang *et al.*) is not satisfied over the entire range of accessible energies, but it is consistent with the existing data at the highest energies, where it holds in various experiments with an accuracy in the range between 3% and 20%.

b) There is still no complete understanding of the precise character of the energy dependence of the inclusive cross sections for reactions with exotic quantum numbers in the fragmentation region or of its relation to the exotic character of the combinations  $ab$ ,  $ab\bar{c}$ , and  $a\bar{c}$ ,

particularly at the highest energies, and these problems require further experimental investigations with good statistics. The energy dependence of inclusive reactions with non-exotic quantum numbers is in agreement with the predictions of Mueller-Regge phenomenology.

c) Factorization of the leading Regge singularities has been confirmed with an accuracy of at least 10% for a number of reactions, and at small momentum transfers it holds with even better accuracy ( $\approx 5\%$ ) up to the CERN ISR energies. However, elastic and inelastic diffraction processes exhibit an appreciable violation of factorization, which shows up clearly for  $|-t| > 0.5$  (GeV/c)<sup>2</sup> and seems to be associated with the anomalous behavior of elastic scattering.

d) It is firmly established that there is a dramatic violation of Feynman scaling in the central region even at the highest CERN ISR energies, which is, however, consistent with the existence of an asymptotic limit as  $s \rightarrow \infty$ . It seems to us that the current status of the energy dependence in the central region is similar to the situation which existed in the case of the total cross sections prior to the discovery of the Serpukhov effect. To detect the very probable deviations from the Regge regime in the central region, it will be necessary to markedly improve the accuracy of the experimental data and to progress to higher energies.

e) Definite progress has been made in establishing a relation between deep inelastic interactions and hadron-hadron interactions in the region of small transverse momenta.

f) It has been demonstrated experimentally that significant numbers of the observed stable particles are produced as a result of resonance decays. The qualitative picture of hadron-hadron interactions is in agreement with the predictions of the naive quark-parton models. To gain a deeper understanding of particle production processes in hadronic interactions, it will be necessary to obtain more complete data on the cross sections for producing various particles, particularly resonances, over the entire range of accessible energies.

The authors are grateful to V. V. Anisovich, A. A. Logunov, M. A. Mestvirishvili, V. A. Petrov, A. N. Tolstenkov, and V. M. Shekhter for many useful discussions. It is a pleasure to thank L. N. Gerdyukov, V. A. Uvarov, and O. G. Chikilev for assistance in compiling the data, and V. A. Baranov, T. S. Kulikova, and G. V. Pavlovskaya for effective help in preparing the illustrations and the manuscript.

## REFERENCES

Unless specified otherwise, references to the experimental data given in the figures can be found in Refs. 12 and 13. In citing references to papers presented at the 18th International Conference on High Energy Physics (Tbilisi, July 15-21, 1976), we give the names of the authors and/or institution or collaboration, the serial number of the paper, and (in parentheses) the number of the paper in the parallel session.

<sup>1</sup>A. A. Logunov, M. A. Mestvirishvili, and Nguen Van Hieu, Phys. Lett. B25, 611 (1967). A. A. Logunov and Nguen Van Hieu, in: Topical Conference on High Energy Collisions of Hadrons, Vol. II, CERN, 1968, 68-7.

- <sup>2</sup>Yu. B. Bushnin *et al.* (IHER-CERN Collaboration), *Phys. Lett.* **B29**, 48; **B30**, 506 (1969).
- <sup>3</sup>D. B. Smith, R. J. Sprafka, and J. A. Anderson, *Phys. Rev. Lett.* **23**, 1064 (1969).
- <sup>4</sup>J. Benecke, T. T. Chou, C. N. Yang, and E. Yen, *Phys. Rev.* **188**, 2159 (1969).
- <sup>5</sup>R. P. Feynman, *Phys. Rev. Lett.* **23**, 1415 (1969).
- <sup>6</sup>K. Zalewski, Rapporteur's talk at the 17th Intern. Conf. on High Energy Physics, London, 1974.
- <sup>7</sup>K. Böckmann, Rapporteur's talk at the Intern. Conf. on High Energy Physics, Palermo, 1975.
- <sup>8</sup>N. A. McCubbin, Rapporteur's talk at the Intern. Conf. on High Energy Physics, Palermo, 1975.
- <sup>9</sup>M. Boggild and T. Ferbel, *Ann. Rev. Nucl. Sci.* **24**, (1974).
- <sup>10</sup>J. Whitmore, *Phys. Rep.* **10C**, 273 (1974).
- <sup>11</sup>V. G. Grishin, *Fiz. Elem. Chastits At. Yadra* **7**, 595 (1976) [*Sov. J. Part. Nucl.* **7**, 233 (1976)].
- <sup>12</sup>P. V. Chliapnikov, Rapporteur's talk at the 18th Intern. Conf. on High Energy Physics, Tbilisi, 1976.
- <sup>13</sup>P. V. Shlyapnikov, Lectures at the 10th Intern. School for Young High Energy Physicists, Baku, 1976.
- <sup>14</sup>A. K. Likhoded and P. V. Shlyapnikov, Review talk at the Intern. Meeting on Multiparticle Processes at High Energies, Serpukhov, 1976.
- <sup>15</sup>T. T. Chou and C. N. Yang, *Phys. Rev. Lett.* **25**, 1072 (1970).
- <sup>16</sup>M. S. Chanowitz and S. D. Drell, *ibid.* **30**, 807 (1973).
- <sup>17</sup>L. D. Soloviev, in: Proc. of the 3rd Intern. Symposium on Nonlocal Field Theories (Alushta, USSR, April 23-30, 1973); in: JINR Communication D2-7161, Dubna, 1973, p. 193; *Pis'ma Zh. Eksp. Teor. Fiz.* **18**, 455 (1973) [*JETP Lett.* **18**, 268 (1973)]; Preprint IHEP 73-105, Serpukhov, 1973. E. Leader and U. Maor, *Phys. Lett.* **B43**, 505 (1973).
- <sup>18</sup>D. P. Roy and R. G. Roberts, Preprint RL-74-022.
- <sup>19</sup>S. Sakai, *Phys. Lett.* **B48**, 427 (1974).
- <sup>20</sup>A. K. Likhoded and A. N. Tolstikov, Preprint IFVÉ 75-57, Serpukhov, 1975.
- <sup>21</sup>Z. Koba, H. Nielsen, and P. Olssen, *Nucl. Phys.* **B40**, 317 (1972).
- <sup>22</sup>V. V. Ammosov *et al.*, Preprint IHER M-26, Serpukhov, 1976.
- <sup>23</sup>K. Yaeger *et al.*, *Phys. Rev.* **D11**, 2405 (1975).
- <sup>24</sup>A. Sheng *et al.*, *ibid.*, p. 17.
- <sup>25</sup>C. Cochet *et al.* (France-USSR and CERN-USSR Collaborations), paper 1034 (A2-89).
- <sup>26</sup>P. V. Chliapnikov *et al.*, *Nucl. Phys.* **B112** (1976).
- <sup>27</sup>D. Bogert *et al.* (FNAL-Florida Collaboration), paper 199 (A2-33).
- <sup>28</sup>D. Bertrand *et al.* (Brussels-CERN-London-Mons-Orsay Collaboration), paper 722 (A2-67).
- <sup>29</sup>B. V. Batyunya *et al.* (Alma Ata-Dubna-Helsinki-Moscow-Prague-Kosice Collaboration), paper 159 (A2-11).
- <sup>30</sup>K. Hanton *et al.* (France-USSR and CERN-USSR Collaborations), paper 1035 (A2-90).
- <sup>31</sup>M. T. Regan *et al.* (Liverpool-Stockholm Collaboration), paper 682 (A2-63).
- <sup>32</sup>P. V. Chliapnikov *et al.* (France-USSR and CERN-USSR Collaborations), paper 1167 (A2-127).
- <sup>33</sup>P. V. Chliapnikov, Invited talk at the Intern. Conf. on High Energy Physics, Palermo, 1975.
- <sup>34</sup>A. Givernaud *et al.* (France-USSR and CERN-USSR Collaborations), paper 1161 (A1-10).
- <sup>35</sup>J. I. Arestov *et al.* (France-USSR and CERN-USSR Collaborations), paper 207 (A2-37).
- <sup>36</sup>A. H. Mueller, *Phys. Rev.* **D2**, 2663 (1970).
- <sup>37</sup>H. I. Miettinen, CERN preprint TH. 2072, 1975.
- <sup>38</sup>A. B. Kaidalov, Rapporteur's talk at the 18th Intern. Conf. on High Energy Physics, Tbilisi, 1976.
- <sup>39</sup>H. M. Chan *et al.*, *Phys. Rev. Lett.* **26**, 672 (1971).
- <sup>40</sup>R. Stroynowski, Rapporteur's talk at the 6th Intern. Colloquium on Multiparticle Reactions, Oxford, 1975.
- <sup>41</sup>T. Ferbel, in: Proc. of the Summer Institute of Particle Physics, Vol. II, SLAC Report 179 (1974), p. 175.
- <sup>42</sup>J. Whitmore *et al.*, *Phys. Lett.* **B60**, 211 (1976).
- <sup>43</sup>H. I. Miettinen, *ibid.* **B38**, 431 (1972).
- <sup>44</sup>G. Ciapetti *et al.*, *Nucl. Phys.* **B89**, 365 (1975).
- <sup>45</sup>E. W. Beier *et al.* (Pennsylvania), paper 402 (A2-59).
- <sup>46</sup>R. K. Garnegie *et al.* (SLAC), paper 289 (A2-55).
- <sup>47</sup>D. Denergi *et al.* (Saclay-École Polytechnique-Rutherford Collaboration), paper 73 (A1-72).
- <sup>48</sup>W. Lockman *et al.* (California-Saclay Collaboration), UCLA-1104, 1976.
- <sup>49</sup>A. K. Likhoded and A. N. Tolstikov, *Pis'ma Zh. Eksp. Teor. Fiz.* **20**, 490 (1974) [*JETP Lett.* **20**, 223 (1974)].
- <sup>50</sup>K. Guettler *et al.*, *Phys. Lett.* **B64**, 111 (1976).
- <sup>51</sup>K. Guettler *et al.*, *Nucl. Phys.* **B116**, 77 (1976).
- <sup>52</sup>B. Apel *et al.*, *ibid.* **B100**, 237 (1975).
- <sup>53</sup>V. Blobel *et al.*, *ibid.* **B69**, 454 (1976).
- <sup>54</sup>P. V. Chliapnikov *et al.*, *ibid.* **B97**, 1 (1975).
- <sup>55</sup>H. Cheng and T. T. Wu, *Phys. Lett.* **B45**, 367 (1973).
- <sup>56</sup>V. V. Ezhela, A. A. Logunov, and M. A. Mestvirishvili, Preprint IHEP 72-1, Serpukhov, 1971.
- <sup>57</sup>M. S. Dubovikov and K. A. Ter-Martirosyan, Preprint ITÉF 37, Moscow, 1976.
- <sup>58</sup>A. Capella and A. Kaidalov, *Nucl. Phys.* **B111**, 477 (1976).
- <sup>59</sup>V. A. Abramovskii, O. V. Kancheli, and I. B. Mandzhavidze, *Yad. Fiz.* **13**, 1102 (1971) [*Sov. J. Nucl. Phys.* **13**, 630 (1971)]. Chan Hong-Mo *et al.*, *Phys. Lett.* **B40**, 406 (1972).
- <sup>60</sup>V. A. Abramovskii, V. N. Gribov, and O. V. Kancheli, *Yad. Fiz.* **18**, 595 (1973) [*Sov. J. Nucl. Phys.* **18**, 308 (1974)].
- <sup>61</sup>M. N. Kobrinskiĭ, A. K. Likhoded, and A. N. Tolstikov, *Yad. Fiz.* **20**, 775 (1974) [*Sov. J. Nucl. Phys.* **20**, 414 (1975)]. A. K. Likhoded and A. N. Tolstikov, Preprint IHEP 74-51, Serpukhov, 1974.
- <sup>62</sup>R. Windmolders *et al.*, *Yad. Fiz.* **22**, 1014 (1975) [*Sov. J. Nucl. Phys.* **22**, 528 (1975)].
- <sup>63</sup>P. V. Chliapnikov *et al.*, Preprint IHEP 76-97, Serpukhov, 1976.
- <sup>64</sup>T. Inami, *Nucl. Phys.* **B77**, 337 (1975).
- <sup>65</sup>E. M. Levin and M. G. Ryskin, *Pis'ma Zh. Eksp. Teor. Fiz.* **17**, 669 (1973) [*JETP Lett.* **17**, 465 (1973)]. A. K. Likhoded and A. N. Tolstikov, *ibid.* **20**, 433 (1974) [**20**, 195 (1974)].
- <sup>66</sup>T. Ferbel, *Phys. Rev.* **D8**, 2321 (1973).
- <sup>67</sup>A. M. Rossi *et al.*, *Nucl. Phys.* **B84**, 269 (1975). Z. R. Babaev and V. I. Koreshev, *Yad. Fiz.* **24**, 429 (1976) [*Sov. J. Nucl. Phys.* **24**, 222 (1976)].
- <sup>68</sup>T. Stewart *et al.* (Durham-Lods Collaboration), paper 194 (A2-29).
- <sup>69</sup>S. N. Vernov *et al.*, paper 778 (A2-110).
- <sup>70</sup>V. P. Pavluchenko *et al.*, paper 169 (A2-2).
- <sup>71</sup>V. K. Budilov *et al.* ("Pamir" Collaboration), paper 169 (A2-1).
- <sup>72</sup>N. N. Roinishvili, Mini-rapporteur's talk at the Tbilisi Conference.
- <sup>73</sup>P. V. Chliapnikov *et al.*, *Phys. Lett.* **B52**, 375 (1974).
- <sup>74</sup>I. V. Ajinenko *et al.*, Preprint IHEP M-30, Serpukhov, 1976.
- <sup>75</sup>V. V. Babintsev *et al.* (France-USSR and CERN-USSR Collaborations), paper 204 (A2-35).
- <sup>76</sup>F. W. Busser *et al.*, *Phys. Lett.* **B46**, 471 (1973).
- <sup>77</sup>D. Sivers, *Nucl. Phys.* **B106**, 95 (1976).
- <sup>78</sup>A. A. Logunov *et al.*, Preprints IHEP 74-66, Serpukhov, 1974; IHER 76-157, Serpukhov, 1976.
- <sup>79</sup>A. N. Tolstikov, paper 791 (A5-2); Preprint IFVÉ 76-51, Serpukhov, 1976.
- <sup>80</sup>P. V. Chliapnikov, in: 4th Intern. Seminar on High Energy Physics Problems, Dubna, 1975, p. 32.
- <sup>81</sup>H. Goldberg, *Nucl. Phys.* **B44**, 149 (1972).
- <sup>82</sup>C. E. De Tar, *Phys. Rev.* **D3**, 128 (1971).
- <sup>83</sup>K. Kinoshita, *Fortschr. Phys.* **24**, 341 (1976).
- <sup>84</sup>P. V. Chliapnikov *et al.*, *Phys. Lett.* **B60**, 218 (1976).
- <sup>85</sup>S. D. Drell and T. M. Yan, *Ann. Phys. (N.Y.)* **66**, 578

- (1971).
- <sup>86</sup>J. F. Gunion, Phys. Rev. **D11**, 1796 (1975).
- <sup>87</sup>R. P. Feynman, Photon-Hadron Interactions, Benjamin, Reading, Mass., 1972 (Russ. Transl., Mir, Moscow, 1975).
- <sup>88</sup>T. K. Gaisser and F. Halzen, Phys. Rev. **D11**, 3157 (1975). D. Sivers, *ibid.*, p. 3253; Nucl. Phys. **B106**, 95 (1976).
- <sup>89</sup>A. K. Likhoded and A. N. Tolstenkov, Preprint IHEP 75-88, Serpukhov, 1975; Yad. Fiz. **24**, 163 (1976) [Sov. J. Nucl. Phys. **24**, 83 (1976)].
- <sup>90</sup>Minh Duong-van, SLAC-PUB-1726, 1976.
- <sup>91</sup>V. V. Anisovich and V. M. Shekhter, Nucl. Phys. **B55**, 455 (1973).
- <sup>92</sup>J. D. Bjorken and G. R. Farrar, Phys. Rev. **D9**, 1449 (1974).
- <sup>93</sup>J. Bartke *et al.* (Aachen-Berlin-Bonn-CERN-Cracow-Heidelberg-Warsaw Collaboration), paper 196 (A2-31).
- <sup>94</sup>A. K. Likhoded, V. A. Petrov, and A. N. Tolstenkov, Preprint IFVÉ 76-2, Serpukhov, 1976.
- <sup>95</sup>U. Gensch *et al.* (France-USSR and CERN-USSR Collaborations), paper 206 (A2-36).
- <sup>96</sup>Scandinavian Bubble Chamber Collaboration, paper 116 (A2-54).
- <sup>97</sup>H. G. Kirk *et al.* (Aachen-Berlin-CERN-London-Vienna Collaboration), paper 695 (A2-68).
- <sup>98</sup>M. De Beer *et al.* (France-USSR and CERN-USSR Collaborations), paper 1168 (A2-128).
- <sup>99</sup>P. V. Chliapnikov *et al.*, Nucl. Phys. **B37**, 336 (1972).
- <sup>100</sup>K. Paler *et al.*, *ibid.* **B96**, 1 (1975).
- <sup>101</sup>Aachen-Berlin-Bonn-CERN-Cracow-London-Vienna-Warsaw Collaboration, paper 663 (A2-105).
- <sup>102</sup>N. N. Biswas *et al.* (Notre Dame-Duke Univ.-Toronto-McGill Univ. Collaboration), paper 1026 (A2-87).
- <sup>103</sup>M. Deutschmann *et al.*, Nucl. Phys. **B103**, 426 (1976).
- <sup>104</sup>Aachen-Berlin-Bonn-CERN-Cracow-Heidelberg-Warsaw Collaboration, paper 664 (A2-104).
- <sup>105</sup>Aachen-Berlin-Bonn-CERN-Cracow-London-Vienna-Warsaw Collaboration, paper 186 (A2-27).
- <sup>106</sup>V. Blobel *et al.*, Phys. Lett. **B48**, 73 (1974); Nucl. Phys. **B69**, 237 (1974); Preprint HE 76-9, Bonn, 1976.
- <sup>107</sup>J. C. M. Armitage *et al.* (CHM Collaboration), paper 347 (A2-72).
- <sup>108</sup>V. Blobel *et al.*, Phys. Lett. **B59**, 88 (1975).
- <sup>109</sup>P. L. Woodworth *et al.*, Preprint CERN E. P. PHYS-76-53, 1976.
- <sup>110</sup>R. A. Donald *et al.*, Phys. Lett. **B61**, 210 (1976).
- <sup>111</sup>Rutherford-École Polytechnique-Saclay Collaboration, paper 71 (A1-70).
- <sup>112</sup>R. Baldi *et al.* (Geneva Univ.), paper 728 (A1-135).
- <sup>113</sup>Yu. M. Antipov *et al.*, Preprint IHEP 76-42, Serpukhov, 1976.
- <sup>114</sup>V. Matveev, R. Muradyan, and A. Tavkhelidze, Lett. Nuovo Cimento **7**, 719 (1973).
- <sup>115</sup>M. L. Mallary *et al.* (Northeastern Univ.), paper 138 (N1-18).
- <sup>116</sup>W. Lockman *et al.* (Univ. California-Aachen-CERN Collaboration), paper 1201 (A2-108).
- <sup>117</sup>M. Bardadin-Otwinowska *et al.*, Nucl. Phys. **B72** (1974).
- <sup>118</sup>P. V. Chliapnikov *et al.*, *ibid.* **B91**, 413 (1975); Phys. Lett. **B55**, 237 (1975).
- <sup>119</sup>H. Voorthuis *et al.* (Amsterdam-CERN-Nijmegen-Oxford Collaboration), paper 277 (C3-24).
- <sup>120</sup>W. J. Robertson *et al.*, Phys. Rev. **D7**, 2554 (1973).
- <sup>121</sup>J. Hanlon *et al.*, FERMILAB-PUB-76/28-EXP, 1976.
- <sup>122</sup>M. Bardadin-Otwinowska *et al.*, Paper submitted to the Intern. Conf. on Elementary Particles, Palermo, Italy, 1975.
- <sup>123</sup>P. V. Chliapnikov *et al.*, Nucl. Phys. **B105**, 510 (1976).
- <sup>124</sup>Aachen-Berlin-Bonn-CERN-Cracow-Heidelberg-London-Vienna-Warsaw Collaboration, paper 198 (A2-32).
- <sup>125</sup>Amsterdam-CERN-Nijmegen-Oxford Collaboration, paper 278 (A2-52).
- <sup>126</sup>Aachen-Berlin-CERN-London-Vienna Collaboration, paper 144 (A2-111).
- <sup>127</sup>M. Bardadin-Otwinowska *et al.*, Nucl. Phys. **B98**, 418 (1975).
- <sup>128</sup>P. Gizbert-Studnicki and A. Golemo, Lett. Nuovo Cimento **6**, 473 (1970).
- <sup>129</sup>Amsterdam-CERN-Nijmegen-Oxford Collaboration, paper 272 (A2-50).

Translated by N. M. Queen